Cross-Reactive Chemical Sensor Arrays

Keith J. Albert,[†] Nathan S. Lewis,*[,‡] Caroline L. Schauer,[†] Gregory A. Sotzing,[‡] Shannon E. Stitzel,[†] Thomas P. Vaid,[‡] and David R. Walt*[,†]

The Max Tishler Laboratory for Organic Chemistry, Department of Chemistry, Tufts University, Medford, Massachusetts 02155, and Division of Chemistry and Chemical Engineering, California Institute of Technology, Pasadena, California 91125

Received August 17, 1999

Contents

I. Introduction

Conventional approaches to chemical sensors have traditionally made use of a "lock-and-key" design, wherein a specific receptor is synthesized in order to strongly and highly selectively bind the analyte of interest.[1−6] A related approach involves exploiting a general physicochemical effect selectively toward a single analyte, such as the use of the ionic effect in the construction of a pH electrode. In the first approach, selectivity is achieved through recognition of the analyte at the receptor site, and in the second, selectivity is achieved through the transduction process in which the method of detection dictates which species are sensed. Such approaches are appropriate when a specific target compound is to be identified in the presence of controlled backgrounds and interferences. However, this type of approach requires the synthesis of a separate, highly selective sensor for each analyte to be detected. In addition, this type of approach is not particularly useful for analyzing, classifying, or assigning human value judgments to the composition of complex vapor mixtures such as perfumes, beers, foods, mixtures of solvents, etc.

An emerging strategy that is complementary to the conventional chemical sensing approach involves the use of sensor arrays. The utilization of sensor arrays is inspired by the superb performance of biological olfactory systems in odor detection, identification, tracking, and location tasks. Recent work has shown that the mammalian olfactory system contains approximately 1000 different olfactory receptor genes and that, upon odor stimulation, responses from many receptors are sent to the olfactory bulb and then on to the olfactory cortex for processing.[7−10] Furthermore, recent experiments have shown that the olfactory receptors are not highly selective toward specific analytes; in fact, one receptor responds to many analytes and many receptors respond to any given analyte.[8,10−12] Pattern recognition methods are thus thought to be a dominant mode of olfactory

[†] Tufts University.
[‡] California Institute of Technology.

10.1021/cr980102w CCC: $35.00
Published on Web 06/24/2000

Keith Albert was born in Lewiston, ME in 1974. He attended Colby College where he did a one year exchange program at UCC in Cork, Ireland. He received his bachelor's degree in 1996 and is presently a graduate student at Tufts University with Prof. David Walt. His research interests include optical sensors, explosives-like vapor detection with microsensor array platforms, and instrumental designs for field use.

Dr. Nathan Lewis has been on the faculty at the California Institute of Technology since 1988 and has served as Professor since 1991. He has also served as the Principal Investigator of the Beckman Institute Molecular Materials Resource Center at Caltech since 1992. From 1981 to 1986, he was on the faculty at Stanford, as an Assistant Professor from 1981 to 1985 and a tenured Associate Professor from 1986 to 1988. Dr. Lewis received his Ph.D in Chemistry from the Massachusetts Institute of Technology. Dr. Lewis has been an Alfred P. Sloan Fellow, a Camille and Henry Dreyfus Teacher–Scholar, and a Presidential Young Investigator. He received the Frensenius Award in 1990 and the ACS Award in Pure Chemistry in 1991. He has published over 170 papers and has supervised approximately 50 graduate students and postdoctoral associates. His research interests include semiconductor electrochemistry and photochemistry, scanning tunneling microscopy of organic monolayers, and artificial olfactory systems using arrays of chemical sensors.

signal processing in the broadly responsive portion of the olfactory system of higher mammals.

In the array approach, the strict "lock-and-key" design criterion of traditional sensing devices is abandoned. Instead, in this alternative sensor architecture, an array of different sensors is used, with every element in the sensor array chosen to respond to a number of different chemicals or classes of chemicals. The elements of such an array need not be individually highly selective toward any given analyte, so this stressing constraint on sensor design is relaxed. Instead, the collection of sensors should contain as much chemical diversity as possible, so that the array responds to the largest possible cross-section of analytes. In practice, most chemical sensors

Caroline Schauer was born in Washington, DC, and graduated in 1991 from Beloit College in Beloit, WI with a B.S. degree in Chemistry. She completed her M.S. and Ph.D. from State University of New York at Stony Brook under the direction of Professors Frank W. Fowler and Joseph W. Lauher working on organic synthesis and small-molecule crystallography. She spent 9 months in the laboratory of David N. Reinhoudt as a postdoctoral fellow at the University of Twente, The Netherlands, working on hydrogen-bonded polymers. Currently she is a postdoctoral fellow in the laboratory of David R. Walt at Tufts University working on enzymatic biosensors. Her research interests include structural chemistry and biology, biosensors for proteins, development of an optical array for the diagnoses of disease states, and crystallography.

Gregory Sotzing was born in Fredericksburg, VA and graduated in 1993 from Mary Washington College with a B.S. degree in Chemistry with highest honors. He received the ACS Polyed Undergraduate Polymer Chemistry Award for his work on the synthesis of fluorinated polyimides. After completing his Ph.D. degree in 1997 under the advisement of John Reynolds in the George and Josephine Bulter Polymer Research Laboratory at the University of Florida, he accepted a postdoctoral position at the California Institute of Technology working jointly with Nathan Lewis and Robert Grubbs. Presently, Greg is an Assistant Professor of Chemistry in the Institute of Materials Science, Polymer Program, at the University of Connecticut, Storrs, CT. His research interests are primarily directed toward the application fields of sensors and actuators with an emphasis on materials design and polymer synthesis (www.mail.ims.uconn.edu/~sotzing).

suffer from some interference by responding to chemical species that are structurally or chemically similar to the desired analyte. This interference is an inevitable consequence of the "lock" being able to fit a number of imperfect "keys". Differentially responsive arrays take advantage of this interference or "cross reactivity" by deliberately attempting to use the nonspecific response patterns for analyte recognition. In this design, identification of an analyte cannot be accomplished from the response of a single sensor element; a distinct pattern of responses pro-

Shannon Stitzel was born in Mons, Belgium, in 1975. She received her B.S. in Chemistry from Davidson College in 1997. Presently she is a graduate student in Chemistry at Tufts University with Prof. David Walt. Her research interests include designing fiber-optic chemical sensors for vapor and liquid-phase analytes and alternative fuel sources.

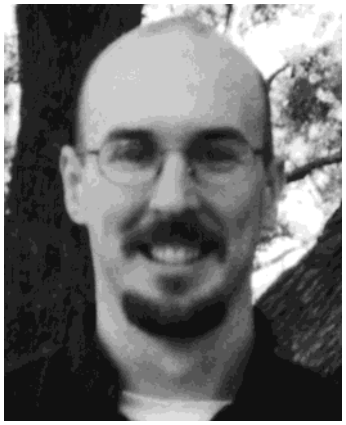

Thomas Vaid was born in 1971 in Elk Grove, IL. He received his B.S. in Chemistry from the University of Illinois at Urbana-Champaign in 1992. His graduate work was with Prof. Peter T. Wolczanski at Cornell University, where he received his Ph.D. in 1997. Since then he has been a postdoctoral scholar at the California Institute of Technology with Prof. Nathan Lewis. In the fall of 2000, he will join the faculty of Washington University in St. Louis as an Assistant Professor in Chemistry. His research interests include the synthesis and study of new inorganic and organic materials with unusual magnetic ordering or electrical transport properties.

Dr. David R. Walt is Robinson Professor of Chemistry at Tufts University. He received a B.S. in Chemistry from the University of Michigan and a Ph.D. in Organic Chemistry and Pharmacology from SUNY at Stony Brook. After postdoctoral studies at MIT, he joined the chemistry faculty at Tufts. Dr. Walt served as Chemistry Department Chairman from 1989 to 1996. Dr. Walt serves on many government advisory panels and editorial advisory boards. He has received numerous national and international awards and honors recognizing his work. Dr. Walt has published over 120 papers, holds over 30 patents, and has given hundreds of invited scientific presentations. His research interests include micro and nano sensors, genomics and organized assembly of nano materials.

duced over the collection of sensors in the array can provide a fingerprint that allows classification and identification of the analyte (Figure 1). The pattern can be obtained from equilibrium or kinetic responses with the latter often providing additional discriminating power. The response mechanism for such systems is highly varied, as described in the sections below. Both binding and colligative properties can be interrogated with such arrays. For example, broadly responsive receptors can be employed to allow a range of structurally similar molecules to bind, membranes may be used that are size selective, and polymers may be employed that select on the basis of polarity. All these recognition mechanisms, as well as others described in this review, are often employed simultaneously in these arrays. These types of systems, which are the topic of this review, are thus commonly designated as artificial or electronic noses.

The advantage of this approach is that it can yield responses to a variety of different analytes, including those for which the array was not necessarily originally designed to detect. An array of sensors naturally performs an integration to yield a unique signal for complex but distinctive odors (e.g., cheeses, beers, etc.) without requiring that the mixture be broken down into its individual components prior to, or during, the analysis. This is a disadvantage when the precise chemical composition of a complex mixture is required but is advantageous when the only required information is the composite composition of the odor of concern. Some additional information can also be obtained by identifying unique spatial and/or temporal characteristics of certain analytes, so that the composition of even modestly complex mixtures can sometimes be obtained from sensor array signals using such methods. Another potential disadvantage to an array system is the possibility that other unknowns may give the same “unique” signal as a specific analyte of interest. However, these arrays are no different from other sensor types, in that there is always the potential for species other than the analyte of interest to provide a response that may be misconstrued as the target analyte. As will be described later in this review, cross-reactive arrays can be trained to evaluate more complex aspects of a sample, such as “freshness”, and the fidelity of such an analysis may pose additional stringencies on the quality of the information produced by the array in order for it to not be “fooled”. The sensors themselves are typically low power and simple in concept and operate at ambient or near ambient temperature and pressure. Their simplicity eliminates the need to solve the power and complexity challenges involved in miniaturizing traditional laboratory analytical chemical systems that involve high power and high vacuum (mass spectrometers, for example), high pressures and/or gas flows (e.g., gas chromatography), or other operational constraints that present severe mismatches between the optimal instrumental operating conditions and those likely to be encountered in an out-of-lab setting.

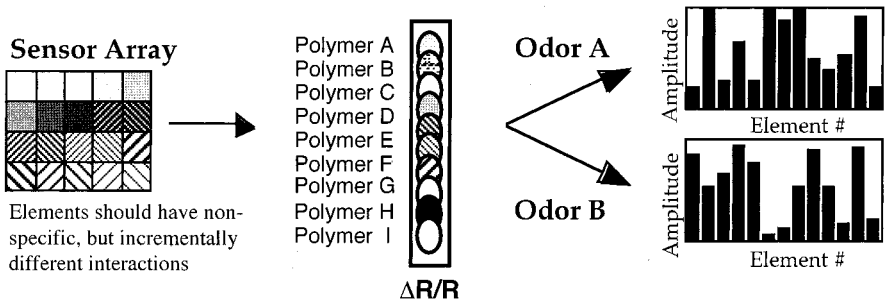

Figure 1. Response of a collection of incrementally different but nonspecific sensors, used to generate a complex pattern, or fingerprint, characteristic of a given analyte. Pattern recognition processing, including neural networks, can then be used to identify analytes on the basis of these patterns.

Signal processing methods and algorithms are intimately associated with the performance of broadly cross-reactive sensor arrays as a vapor detection system. Signal processing algorithms can comprise statistically based chemometric methods, pattern recognition algorithms, neural networks, or some combination thereof. One of the design tradeoffs in deploying any specific sensor array system for a given vapor detection task will thus clearly involve assessment of the computational needs to achieve a robust classification of the desired target analyte in the presence of background, environmental variability, and interfering signals.

There is some controversy in the literature regarding whether it is advantageous to use large numbers of sensors in an array device. This arises because approximately five fundamental molecular descriptors have been sufficient to describe much of the variance in the gas−solid partition coefficients for sorption of vapors into various polymers. Although it is possible to describe the gross features of such partitioning with a small number of descriptors, we note that there are over 1000 olfactory genes in humans and over 100 million olfactory cells in a canine's nose. Even if the dimensionality of odor space is fairly small, say on the order of 10^1, it is not likely that ideal sensors that produce optimal resolution along the fundamental directions of odor space could be identified. In practice, correlations between the elements of a sensor array will likely necessitate a much larger number of sensors to distinguish successfully between any two molecules in a complex environment. Also, it is beneficial to measure the same property in many different ways due to noise limitations in a practical system. For example, if sufficient precision could be obtained, it might be possible to identify uniquely any molecule merely from a 38 bit precision measurement of two parameters, perhaps its dipole moment and its polarizability. But of course, it is not practical to make such measurements with this precision; hence at lower precision, useful information on the nature of the analyte is gained by making measurements of the molecular parameters through many independent determinations on different sensor elements. The dimensionality of odor space will depend on the sensor array and the recognition mechanism employed. The dimensionality of odor space is thus inherently coupled to the precision of the sensor array that is being used to make the determination as well as to the diversity in the analytes that is being used to define the space as a whole. Furthermore, the above arguments on needing a limited number of sensors only hold if one is tasked to distinguish between a series of pure substances that are maintained at one fixed, known concentration. In contrast, if the background is unknown, if mixtures are present, or if the background gases are changing in concentration, many more sensors are needed simply to avoid ambiguity in interpreting the output signal pattern, and even more are needed if optimal discrimination is to be accomplished between a given target signature and a wide possible range of background clutter and false alarm signatures. Having large numbers of sensors also allows redundancy, which improves the signal-to-noise ratio and provides the ability to veto the output of poorly performing sensors. Redundancy is clearly important in biological systems where each odorant receptor type is expressed clonally on thousands of individual cells. Because of all of these issues, the number of sensors required to successfully span odor space in a practical device will rapidly multiply from the minimum value defined by the rank of smell space, and this is a requirement that is readily met using versatile sensor array architectures that can incorporate high levels of chemical diversity and redundancy into the system.

Sensor types for electronic noses can be quite diverse. Sensor array elements that will be discussed in this review include metal oxide devices, intrinsically conducting organic polymers, conducting polymer composites, dye-impregnated polymers coated onto optical fibers, electrochemical devices, and polymer-coated surface or bulk acoustic wave oscillators. While the focus of this review is primarily on the chemistry of these arrays, there are a number of application areas for the technology that will be of interest to the reader. These cross-reactive arrays have a wide variety of application areas including food and beverages, fragrances, environmental monitoring, chemical and biochemical processing, medical diagnostics, transportation, and a host of others. Some aspects of these areas as well as specific examples from each will be illustrated in the appropriate sections of the text that follows.

II. Tin Oxide Arrays

A. Theory

Tin oxide (SnO_2) gas sensors were first demonstrated in the early 1960s. Since that time, SnO_2

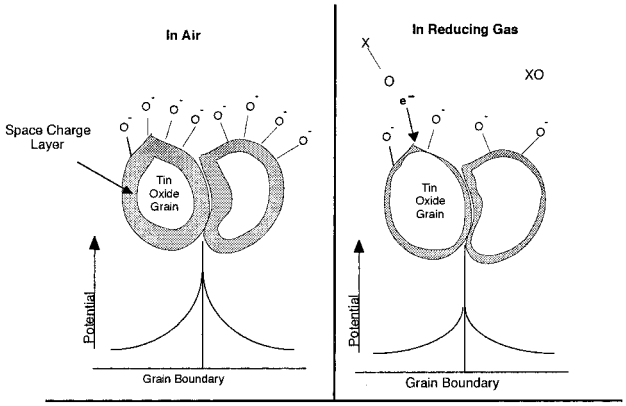

Figure 2. Potential barrier at the grain boundary (a) in air and (b) in a reducing gas.

sensors have become commercially available for detecting fuel gas, carbon monoxide, general purpose combustible gases, ammonia, water vapor, etc.[13,14] As early as 1954, the concept of a cross-reactive array of sensors for odor detection was discussed in the literature.[15] However, it was not until 1982 that a cross-reactive array of SnO_2 sensors was demonstrated by Persaud and Dodd to mimic olfaction.[16] This publication started the "modern era" of cross-reactive arrays and electronic noses that combine broad sensitivity with convergent signal processing to perform a wide range of analyte identification. Although many different arrays have been fabricated, the sensing mechanism is similar for all SnO_2 elements.

The general mechanism for vapor sensing with tin oxide is a change in the resistance (or conductance) of the sensor when it is exposed to an analyte relative to the sensor resistance in background air. This change in resistance is due to irreversible reactions between the analyte and oxygen-derived adsorbates such as O^-, O_2^-, and O^{2-} on the semiconductor surface. The most reactive of these species is O^-, which tends to dominate the resistance of the semiconductor through chemical control of vacancy sites in the SnO_2. Oxygen adsorbs to the semiconductor surface according to the following equation:

$$^1/_2O_2 + e^- \rightarrow O^- \text{ (ad.)} \qquad (1)$$

With n-type semiconductors, adsorption of O^- creates a space-charge layer on the surface of each SnO_2 grain, which creates a potential barrier to conduction at each grain boundary. The depth of the space charge layer changes in relation to the concentration of oxygen adsorbates on the surface. Therefore, when the surface is exposed to air, the oxygen concentration is high and the material displays a high electrical resistivity. In contrast, when the sensor is exposed to a reducing gas X, the gas reacts with some adsorbed oxygen species O_m^- as follows:

$$X + O_m^- \rightarrow XO_m + e^- \qquad (2)$$

This leads to oxygen consumption, the return of electrons to the oxide grains, and a decrease in the semiconductor resistance (Figure 2). When the sensor is exposed to an oxidizing gas such as NO_2, the resistance increases as the gas chemisorbs as a negatively charged species to the semiconductor surface. The change in resistance is therefore due to the chemisorption of the oxidizing gas, assuming that the concentration of oxygen adsorbates remains constant.[13,14,17] Another hypothesis for the mechanism of conductivity change in SnO_2 is that reducing gases react with the material and thereby reduce the number of oxygen vacancies in the material, lowering its conductance, while oxidizing environments regenerate the oxygen-derived vacancies and thus restore the electrical conductivity of the film.

B. Tin Oxide Characteristics

Various properties of tin oxide arrays have been manipulated in attempts to enhance and/or broaden the sensitivities of such devices. The sensitivities of SnO_2 sensors to various gases can be enhanced by doping with metals. Metals promote the catalytic activity of the semiconductor surface with gases, leading to chemical sensitization. The addition of a metal to SnO_2 also causes electronic sensitization due to the effects on the space charge layer. Metals that have work functions greater than the electron affinity of the semiconductor take electrons from the semiconductor, leading to even greater resistances in air. Because oxygen adsorbs to both the metal and semiconductor surfaces, when it desorbs from both surfaces due to gas interactions, an enhanced sensitivity is produced in the resistance change of the semiconductor.[14] Typical doping metals include Pt and Pd, but others have also been used, such as Al[18] and Au[19] (although neither Al nor Au has provided much improvement in sensitivity). Doping with Pt and Pd has been shown to increase the sensitivity of tin oxide sensors to gases such as benzene and toluene, with lower doping concentrations leading to greater sensitivity. Doped sensors have demonstrated greater sensitivity to oxygenated volatile organics than to aliphatic, aromatic, or chlorinated compounds.[18]

Temperature is another factor that affects the sensitivity of tin oxide sensor arrays. Typically, these arrays are operated at temperatures greater than 300 °C to increase the reactivity of the semiconductor surfaces. Tin oxide sensors are also operated at elevated temperatures to desorb water produced from the reactions on the catalyst surface. One study looked at the effect of various temperatures between 300 and 450 °C on an array of three elements.[20] It was determined that if a sensor's response changed linearly with change in temperature, it did not affect the array's overall performance. An approach to utilize the change in sensitivity with temperature is to use a thermal cycling technique to extract more information from each sensor. This approach was first demonstrated by Heilig et al.[21] and then used by Corcoran et al., who cycled an eight sensor array between 250 and 500 °C. These workers used the data in conjunction with feature extraction techniques to classify teas. The thermally cycled array had a 90% classification rate, whereas the same array at a fixed temperature only had a 69% classification rate.[22]

Another study investigated the response and recovery times of tin oxide sensors.[19] Some general conclusions could be drawn, for example, that as analyte concentration increased, response time decreased while sensor recovery times increased. For concentrations between 0 and 400 ppm, the response times varied from 5 to 35 s, while recovery times ranged from 15 to 70 s, depending on the analyte. A comparison between tin oxide, conducting organic polymers and carbon-black polymers found that tin oxide sensors responded more quickly (~7 s) than the other sensor types (20−200 s). Tin oxide sensors were also found to have larger responses in general but were not found to be as good at resolving volatile organic compounds as carbon black−polymer composites.[23]

C. Array Design

The first array developed with tin oxide sensors used commercially available sensor elements (Figure 3).[16] A typical commercially available element has a

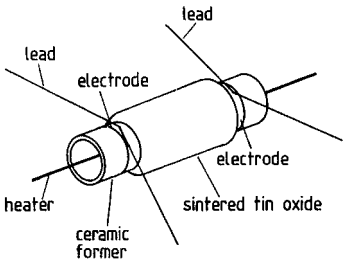

Figure 3. Diagram of the typical commercially available tin oxide gas sensor.

thick film of SnO_2 on a ceramic tube. A heater runs through the center of the tube, and electrical contacts are provided at both ends. Each sensor is individually packaged and is ~1 cm in diameter.[13,17] Commercially available elements are the most widely used SnO_2 array format described in the literature because such sensors are easy to obtain and have a broad range of sensing properties. An example of the Warwick nose, with 12 SnO_2 sensors in the array, is shown in Figure 4.

Tin oxide arrays can also be fabricated on microchips trough silicon-based microfabrication technology to make many identical and miniaturized sensors (Figure 5). Silicon technology allows control over chip array size, power consumption, and sensor reproducibility.[24−26] It also allows for several types of metal oxide layers to be combined within an array.[27,28] In light of the microfabrication technology available, a new design for an array has been developed with built-in circuitry in proximity to each array element. This circuitry performs preprocessing for pattern recognition by using analogue VLSI to translate the sensor inputs to a binary digital output.[29−31] The most recent version has an output generated by using the mean and median values of all sensors, comparing each individual sensor response, and assigning a 1 or 0 corresponding to a high or low value relative to the mean/median. This system was able to discriminate between acetone, butanol, ethanol, methanol, and xylene.[31]

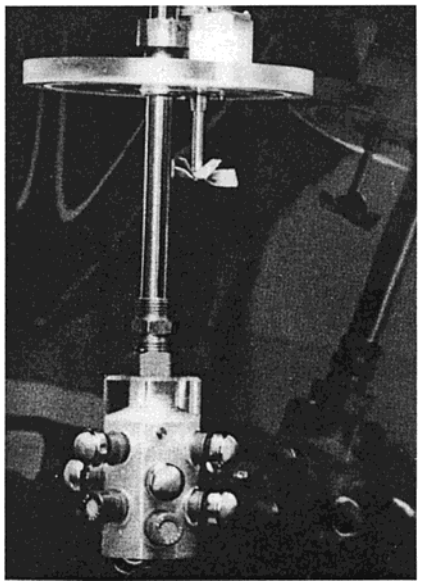

Figure 4. The Warwick Nose, an array of 12 commercially available SnO_2 sensors. Reprinted from *Sens. Actuators B*, Vol. 1, Shurmer, H. V., et al., Intelligent Vapour Discrimination Using a Composite 12-Element Sensor Array, pp 256−260, Copyright 1990, with permission from Elsevier Science.

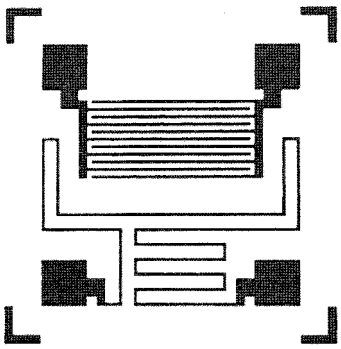

Figure 5. Pattern for interdigitated electrodes (top) and heater (bottom). Reprinted from *Sens. Actuators B*, Vol. 4, Gardner, J. W. et. al., Integrated Tin Oxide Odour Sensors, pp 117−121, Copyright 1991, with permission from Elsevier Science.

One drawback to tin oxide array fabrication is the necessity of incorporating a heating element to operate the array at high temperatures. To avoid this, an array that can operate at room temperature has been demonstrated by treating the sensor elements with an oxygen plasma. When the semiconductor surface is exposed to an oxygen plasma, which has many oxygen species present including both positively and negatively multiple charge species, the SnO_2 surface is covered with a high concentration of oxygen that then reacts with gases and allows sensitivity at room temperature. An untreated array has mostly O^-, O_2^-, and O^{2-}, adsorbed which are mainly unreactive at room temperature. It was found that the plasma-treated array was sensitive to carbon monoxide, carbon tetrachloride, methanol, and light petroleum gas at room temperature, whereas the untreated array was not.[32,33]

D. Applications

Tin oxide sensor arrays have been used to detect a variety of different analytes under varying conditions.

Three major groups of analytes for these arrays are toxic gases,[19,20,32,34,35] volatile organic compounds (VOCs),[16,18,23,30,31,36−42] and food-related species.[22,29,43−53] Toxic gases and VOCs are important components of industrial emissions, and monitoring such analytes can be challenging with a single sensor approach due to drift and interferences. Food analysis benefits from cross-reactive arrays because the technique is noninvasive and does not require breaking down a complex mixture into its individual components merely to establish whether the sample has changed or not from a prior batch.

Work with tin oxide arrays began with VOC's when Persaud and Dodd used compounds such as methanol, ethanol, and diethyl ether to demonstrate that an array of cross-reactive sensors could discriminate between odors without being analyte-specific.[16] Abe showed that with an array of eight sensors, 30 different VOCs could be classified into four categories, ethereal, ethereal-minty, pungent, and ethereal-pungent, on the basis of the odor.[36] Work with volatile organics has continued and is directed toward the more difficult task of analyzing mixtures of organics such as benzene, toluene, octane, and propanol.[37] An array of SnO_2 sensors with a humidity sensor was used to detect and quantify mixtures of methane and ethanol in a variable humidity environment for domestic cooking applications.[54] Arrays for the detection and quantification of sulfides, sulfur oxides, and nitrogen oxides have also been investigated.[34,35]

The use of tin oxide arrays for food and beverage classification is well established. These arrays have been applied to evaluate fish freshness on the basis of various alcohols and biogenic amines given off as fish spoils. A SnO_2 array was shown to have similar sensitivities to fish spoilage as chemical and electrical methods.[49] Coffee beans have been classified on the basis of their aromas, and one study was able to discriminate between different blends of coffee beans as well as to differentiate between various roasting times.[47] SnO_2 arrays have also been used to determine the ripeness of bananas. Llobet et al. were able to classify bananas into seven categories of ripeness on the basis of the headspace sampling of stored bananas.[48]

Various beverages have also been investigated with tin oxide arrays. Di Natale et al. were able to discriminate 1990, 1991, and 1992 vintages of one type of wine.[44] This task was accomplished using a metal oxide-sensing array, with three of the five elements being SnO_2 sensors, and the data were processed with principal component analysis. These workers then used a five-element SnO_2 array to determine which vineyard a particular type of wine had come from, and the method was found to be superior to current standard methods of analysis.[45] In another study, a thermally cycled, eight-sensor array in combination with an artificial neural network was able to discriminate between three different teas.[22]

E. Analysis

Many different parameters affect the outcome of a data analysis process. Some of the key features for tin oxide arrays are the type of signal used for analysis and the normalization process used on these signals before processing and classification is performed. Gardner found that using the fractional conductance gave improved results compared to using the relative or log absolute conductance changes.[55] Other studies have found that using transient signals combined with steady-state signals gives improved discrimination ability in the final processing.[30,39] Preprocessing algorithms can also have important effects on the analysis outcome. For example, by development of a microscopic model of conduction for the array, the appropriate sensor response parameters were selected to improve analyte classification. The normalization procedure developed is shown in eq 3, where S_{ij} is the fractional conductance of the

$$\tilde{S}_{ij} = S_{ij}/(\sum_{i=1}^{n} S_{ij}^{2})^{1/2} = \alpha_{ij}/(\sum_{i=1}^{n} \alpha_{ij}^{2})^{1/2} \qquad (3)$$

ith sensor element to the j_{th} gas and α_{ij} is the ratio of the reaction rates between oxygen desorption and oxygen reaction with gas j. This normalization procedure removes the effect of a change in sign of S_{ij}. A 12-element array was used to distinguish between types of alcohol, including two lagers, two beers, and two spirits. Cluster analysis (CA) of the original data could not separate the lagers from the beers. However, by choice of the appropriate normalization technique, the CA and principal component analysis (PCA) results were enhanced compared to the original results, with lagers and beers being clearly separated.[46]

Chemometric techniques such as principal component analysis, cluster analysis, and least squares methods have been used as techniques to process responses from multianalyte arrays. Using a 12-sensor tin oxide array, discrimination between methanol, ethanol, propan-2-ol, and butan-1-ol was achieved through use of a weighted fault-tolerant least-squares analysis method.[40] A study to evaluate PCA, CA, and partial least squares (PLS) showed that each method was a useful chemometric technique for classifying analytes.[41] Another version of cluster analysis, called transformed cluster analysis (TCA), uses transformation equations based on the mean and variance values for the training data set. This analysis was tested with a four-element metal oxide-sensor array using four individual VOCs, and was found to correctly cluster these analytes.[56] With use of PCA and CA and creation of star symbol plots of sensor array responses to VOCs, it was found that these techniques could help in the development of sensor devices by identifying which sensors provided useful or redundant information.[38,42] The ability to select sensors is useful for creating arrays that can perform specific tasks and also for creating more diverse sensor arrays within the practical constraints of a limited sensor count being available in a fielded device.

A different approach to multianalyte array analysis is to use artificial neural networks (ANN) to perform the data analysis. These systems can handle highly nonlinear data and can deal with noise or sensor drift

with less of a negative impact than classical approaches such as PCA and PLS.[55] As with most data analysis approaches, there are many variations on the ANN theme. Back-propagation networks have been useful to discriminate between similar analytes[39,55] and to analyze gas mixtures containing hydrogen, methane, and carbon monoxide.[57] Self-organizing artificial neural networks (SOM) create unsupervised, statistical descriptions of the environment with no supplementary information. These systems have been shown to perform gas classification well and have been investigated for their ability to learn while operating and thereby counteract sensor drift.[58,59] Fuzzy logic has been incorporated into some neural networks to provide them with the ability to give more than just a yes or no response. This type of neural net in combination with a six element, tin oxide array has been shown to discriminate between carbon monoxide, ethanol, and methane.[60] Fuzzy ARTMAPs seem to be superior to back-propagation networks and learning vector quantization, due to their ability to learn incrementally without forgetting previous information. This feature combined with the ability to classify as well or better than these other techniques could make fuzzy neural nets the best choice for cross-reactive SnO_2 array analysis.[48]

III. MOSFET Arrays

A. Principles of Operation

Metal oxide semiconductor field effect transistors (MOSFET) have been studied as sensors since 1975 when Lundstrom et al. reported a hydrogen-sensitive MOSFET with palladium as the gate metal.[61] These gas sensitive MOSFETs are sometimes referred to as GASFETs. In GASFETs, the structure is the same as a MOSFET, but the traditional aluminum gate is replaced with a catalytically active metal. Since 1975, a significant amount of research has been directed toward finding the best materials for the gate to give better sensitivity and selectivity for a variety of analytes. Several other variations on MOSFETs have been developed, such as open gate field effect transistors (OGFET), ion sensitive field effect transistors (ISFET) (which have an electrolyte solution as the conducting layer), and CHEMFETs (which are ISFETs coated with an organic membrane).[62,63] Although many variations on MOSFETs have been developed, the GASFET seems to be the only type that has been fabricated into cross-reactive arrays.

The MOSFET structure consists of a metal gate on top of an oxide layer, typically SiO_2, and a p-type silicon base with n-doped channels on either side of the gate (Figure 6). The surface potential, φ_s, of the semiconductor layer is dependent on the applied gate voltage V_G and the work function of both the metal, W_m, and semiconductor, W_s, materials.

$$\varphi_s = f_1(V_G - W_{ms}/q) \qquad W_{ms} = W_m - W_s \quad (4)$$

According to eq 4, a change in W_{ms} leads to a change in the surface potential. Therefore, to maintain a constant surface potential, the applied gate voltage must be adjusted in relation to the change in the work function.[62,64]

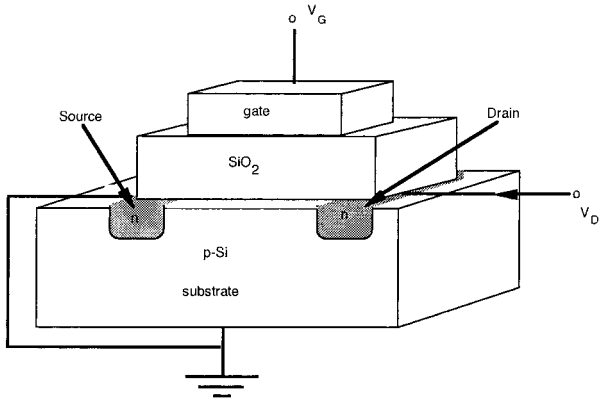

Figure 6. Typical MOSFET structure.

GASFETs operate on the principle that the work functions of the metal and semiconductor are affected by gases adsorbed to the surfaces. The manner in which the W_{ms} is affected depends on whether the metal gate is continuous (thick film) or discontinuous (thin film). On a continuous surface, the metal surface catalyzes dehydrogenation reactions of hydrogen-containing gases using O_2 as the electron acceptor. The hydrogen adsorbs to the metal surface and can diffuse through the metal to the SiO_2/metal interface where a dipole layer is created. The hydrogen dipole layer leads to a change in W_{ms}. On a discontinuous surface, changes are due not only to a hydrogen dipole layer but, in addition, the work function is affected by adsorbates on the metal surface and on exposed portions of the SiO_2 layer.[62,64]

B. Fabrication and Operation

Although many variations on the actual fabrication details for MOSFET sensor arrays are possible, some guidelines are generally followed. Dry oxidation at 1100−1200 °C is first used to create an oxide layer ∼100 nm thick.[65,66] The gate metal can be thermally evaporated onto the oxide surface through a mask, to produce either a layer ∼100−400 nm thick or an ultrathin metal 3−30 nm in thickness.[65,67] The distance between the *n*-regions of the gate is usually 1−10 μm, while the gate depth is between 10 and 100 μm. The actual design of the array can vary significantly, depending on the application. Arrays have been designed with 2−12 MOSFET sensors, and some hybrid arrays have been made with MOSFETs and other sensors (such as tin oxide sensors) combined into the same array.

It is well-known that the type of gate metal as well as the temperature at which the MOSFET is operated will affect the catalytic properties of the sensor. Platinum, palladium, and iridium are the three most common catalytic metals used as gate materials. Pd is a good hydrogen sensor, while Pt and Ir have sensitivities for analytes such as ammonia and ethanol. Modifying the device operating temperature can sometimes enhance the catalytic activity of a sensor toward particular analytes. For example, Pt has a higher affinity for ethylene at 200 °C than at 100 °C (Figure 7).[64]

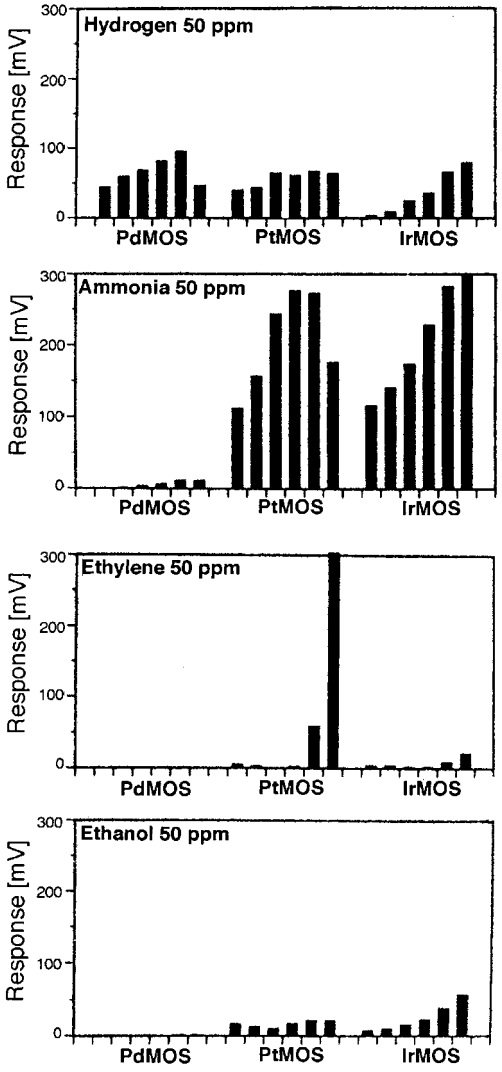

Figure 7. Responses of GASFETs with different gate metals ~100 nm Pd, ~5 nm Pt, and ~5 nm Ir. Each device type was tested with four analytes at 50 ppm in synthetic air and at six temperatures: 75, 100, 125, 150, 175 and 200 °C running from left to right in the diagrams. The responses are the change in gate voltage during a 5 min vapor pulse. Reprinted from ref 64 with kind permission from Kluwer Academic Publishers.

C. Applications

One of the early MOSFET arrays was developed by Muller and Lange and consisted of four palladium gate MOSFET elements. Three of the four elements had zeolite layers with different pore sizes deposited on top of the Pd gate. This array was used to identify hydrogen, methane, and acetylene on the basis of the characteristic changes in capacitance with time. By using correlation coefficients, the three different gases could be classified, regardless of concentration. This approach was only used with single-component gas samples.[66] Muller modified the array to identify binary mixtures of hydrogen and methanol vapors. The cross-sensitivity of a single sensor was compared to the sensitivity of a two element, Pd and Pt MOSFET array. Using the transformed least-squares method, the cross-reactivity patterns of the array could be deconvoluted to determine the concentration of hydrogen within the binary mixture.[68]

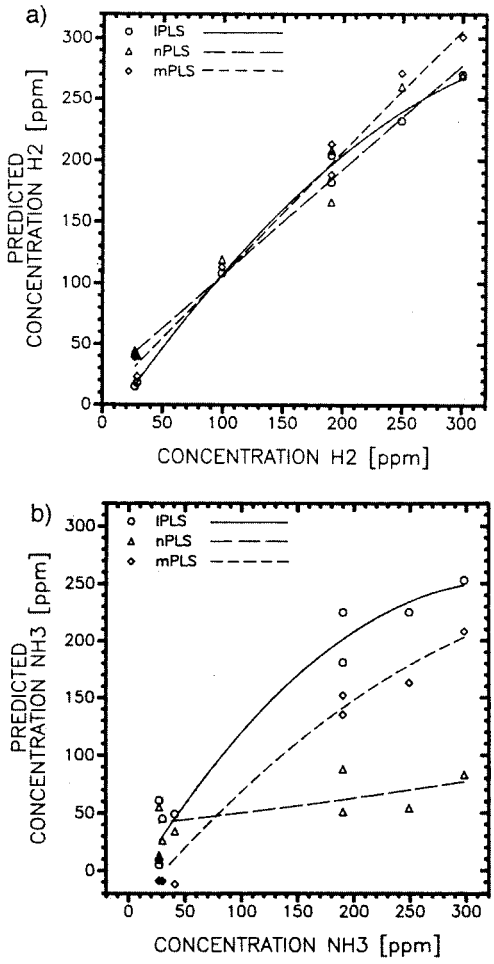

Figure 8. Predicted vs actual concentration of (a) H_2 and (b) NH_3 for the 1PLS, nPLS, and mPLS models. Reprinted from *Sens. Actuators B*, Vol. 2, Sundgren, H., et al., Evaluation of a Multiple Gas Mixture with a Simple MOSFET Gas Sensor Array and Pattern Recognition, pp 115−123, Copyright 1990, with permission from Elsevier Science.

Much of the work with MOSFET cross-reactive arrays has been performed at the Linköping Institute of Technology in Sweden. In 1990, Sundgren et al. showed that an array of commercially available MOSFETs could be used to identify components in a quaternary mixture of gases. The six-element array used in that work consisted of three pairs of Pd and Pt MOSFETs, with each pair operated at different temperatures, 100, 150, and 200 °C. The array was tested with a mixture of hydrogen, ammonia, ethylene, and ethanol in a carrier gas of air and argon. The change in the gate voltage due to exposure of the array to the gas mixtures was monitored over time. The three characteristics of this curve used for analysis were the difference between the pre- and post-exposure values of the gate voltage, the maximum positive derivative, and the maximum negative derivative of the signal with time. Data were analyzed by using three different versions of partial least squares. Using these methods, the concentration of hydrogen and ammonia in the gas mixtures could be predicted, while ethanol and ethylene could not be separated.[67] Figure 8 shows the predicted vs actual concentrations of hydrogen and ammonia with

the three versions of PLS. A 45° line through the origin represents a perfect prediction.

An essential aspect to any type of cross-reactive array is the pattern recognition method employed to determine the composition of the analyte. One study by Sundgren et al. compared the analysis of two types of MOSFET arrays with PLS and an artificial neural network (ANN). The first array was identical to the previously described array[67] and was tested with a mixture of hydrogen, ammonia, ethanol, and ethylene. PLS was able to predict the concentrations of hydrogen and ammonia. ANN could not achieve accurate predictions for ethanol or ethylene either but made closer predictions to the true concentrations of hydrogen and ammonia than PLS. The second test was to use a six-element array consisting of three types of gate materials, Pt, Pd, and Ir. This array was tested with a binary mixture of hydrogen and acetone. Both PLS and ANN were able to make reasonable predictions of the hydrogen and acetone concentrations in these mixtures, with ANN again giving the more accurate prediction. Although ANN was more accurate than PLS in both tests, the authors warned that this might not be the general case.[69]

One other data analysis technique was used with the previously described two type array data.[69] An adaptive learning network using the abductory induction mechanism (AIM) was used to predict the hydrogen and ammonia concentrations. This method was found to have similar prediction capabilities as PLS and ANN, but it was unable to predict the concentration of ethanol and ethylene. This software is relatively fast because it develops the networks in a feed-forward fashion that allows for faster learning than feed-backward ANNs. AIM was found easier to use than PLS or ANN to ascertain which sensor information is being used for each analyte. Since each analyte has its own network, this method of analysis is well suited for analyzing single components of a mixture.[70] A later comparison of ANN and AIM points out that while AIM is faster, ANN can provide a more accurate prediction over a wider concentration range.[71]

D. Alternative Implementations of MOSFETs

Lundstrom et al. have also taken a completely different approach to MOSFET arrays by employing a method called the scanning light-pulse technique.[64,65,72,73] The premise of this approach is that when light is shined on the surface of a MOSFET coated with a thin metal film, the light will penetrate the metal and induce a photocapacitive current (i_{ph}) in the semiconductor. The depletion layer determines this current similar to the surface potential. To maintain a constant i_{ph}, the applied gate voltage must be varied in response to changes in the W_{ms}, just as it would to maintain a constant surface potential. Therefore, when the change in the gate voltage is monitored a map of $\Delta V(x, y)$ over the sensing surface can be obtained by taking the difference between the gate voltage in air vs in gas at the same i_{ph}. In this approach, the MOSFET array employed three continuous strips of Pt, Pd, and Ir along a 4 mm × 6 mm rectangle, instead of separately defined sensor elements. The sensor surface was divided into an 18 × 18 grid, and a temperature gradient (110−180 °C) was established down the length of the sensor surface. This temperature variation allowed for different sensitivity and selectivity at each point of the sensor grid. Hydrogen, ammonia, and ethanol were tested individually as mixtures with air. The change in voltage (ΔV) was determined for each point of the sensor grid, and the plot of ΔV for each gas was then processed by taking the average of the ΔV for each point and its eight nearest neighbors. An average higher than 65 mV was assigned white, and lower averages were assigned black. In this manner, three distinct image maps of the gases were created (Figure 9). The possible uses for such image mapping include gas mixture identification, investigation of new sensing materials simultaneously with the same gas sample, and mapping spatially inhomogeneous reactions.[64,65]

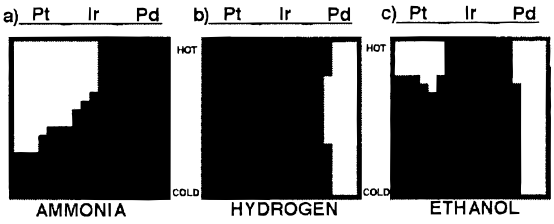

Figure 9. Image maps of (a) ammonia, (b) hydrogen, and (c) ethanol. Reprinted from *Sens. Actuators B*, Vol. 6, Winquist, F., et al., Visual Images of Gas Mixtures Produced with Field-Effect Structures, pp 157−161, Copyright 1992, with permission from Elsevier Science.

Light-pulsed sensing combines many types of information, including the catalytic activity of the gate metals, gas flow turbulence, edge effects, etc. Distributed chemical sensing was inspired by the light-pulsed technique but sought to separate only the effects of catalysis. A cell was designed with a continuous catalytic surface of Pd, with seven MOSFET sensors spaced 2.8 mm apart along the length of the cell. The top and/or bottom of the cell were coated with thick Pd layers and served as continuous catalytic surfaces along the length of the cell. Hydrogen and ethanol were mixed with O_2 and N_2 and were passed through the cell at a constant flow of 10 mL min^{-1}. The monitored response was the change in gate voltage prior to gas exposure and at the end of a gas exposure. Ethanol and hydrogen could be discriminated on the basis of their different catalytic profiles by using information only from the first and last sensors in the cell.[74] A recent paper on distributed chemical sensing utilized two types of MOSFETs and two catalyst surfaces for a total of four different sensor/catalyst combinations. Each array had five identical MOSFET sensors evenly distributed along the length of the cell. The four different array combinations were tested with a quaternary mixture of hydrogen, ammonia, ethyne, and ethanol. Information from all four array types were combined and analyzed with PCA and ANN, and used to estimate all four components of the gas mixture. It was also found that using information from various positions in the cell afforded improved results compared to using only the first and last sensors of the arrays.[75]

E. Hybrid Metal Oxide Containing Arrays

Since the early 1990s, interest has been increasing in creating hybrid arrays, or arrays that combine more than one type of sensing element. Some of these hybrid arrays are already commercially available as electronic noses. Alpha MOS sells The Fox system which is a hybrid array of tin oxide, conducting polymer, and thickness shear mode (TSM) sensors.[76] Another nose available is the eNOSE 5000 from EEV Limited, which consists of conducting polymer, metal oxide, and TSM sensors.[77] In the semiconductor-based sensing area, combining MOSFETs and tin oxide sensors has been especially popular. A common hybrid array setup is using ten MOSFETs, four tin oxide, and one CO_2 sensor. At Linköping University these types of arrays have been used to investigate various food products. For example, these arrays were used to both estimate the storage time of ground pork and beef and to tell these two meats apart.[50,52] Ninety percent of the wheat, barley, and oat samples tested were correctly classified as good or bad based on the mold/musty smells of the grains. This classification rate exceeded the agreement of the two grain inspectors who originally classified the grains.[53] They have also used this array to classify five different types of cardboard, although the best discrimination was found using only 4 of the 15 sensor elements.[78] Recently, this 15-element hybrid array format was used to monitor the different stages of recombinant bioprocesses. The array followed the cultivation of mammalian cells secreting the blood coagulant factor VIII. In combination with PCA, four different stages of the process were determined, being cell growth, draining the reactor, growth medium exchange, and production of blood coagulant.[79]

A slightly smaller hybrid array of eight FETs and four tin oxide sensors combined with a neural network was able to identify 9 out of 10 different types of cheese correctly.[52] A modular approach to hybrid arrays was presented by Ulmer et al. and utilized a variety of sensors such as MOSFET, tin oxide, TSM, and electrochemical sensors. This system was demonstrated to discriminate between different olive oils, whiskeys, tobaccos, coffees, and plastics.[51] A recent paper from the Linköping University has utilized a hybrid array in parallel with a conductive polymer array. A 32-element conductive polymer array was used in parallel with a hybrid array comprised of 10 MOSFETs and 6 tin oxide sensors. This parallel array was used to predict the fermentation of wood hydrolysates and to estimate quantities of components of the hydrolysates. Although some success was demonstrated, the problem was nontrivial.[80]

IV. Intrinsically Conductive Polymer Chemiresistor Arrays

A. Principles of Operation

The experimental and theoretical behaviors of intrinsically conducting polymers (ICP's) have been discussed in several reviews and books,[81−84] so only the basic properties of ICP's that are required to understand the operation of ICP-based sensor arrays are discussed in this section. Typically, the fundamental structural unit of an ICP is a linear backbone comprised of repeating conjugated organic monomers such as acetylene, pyrrole, thiophene, or aniline (Figure 10).

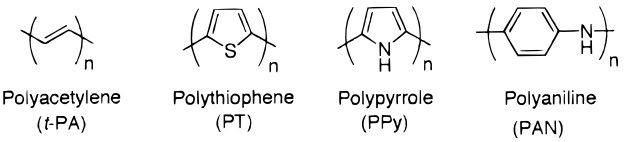

Figure 10. Structure of four intrinsically conductive polymers in their insulating form.

These materials are insulating in their neutral state. However, chemical or electrochemical reduction (n-doping) or oxidation (p-doping) of these materials renders the polymers electrically conductive. The conductivity is produced through band structure transformation and/or the generation of charge carriers. A vast majority of ICPs act as one-dimensional conductors because the electrons in an n-type ICP (or holes in a p-type ICP) mainly travel through the linear conjugated chains. Formally, the materials are usually electrical semiconductors as opposed to metallic conductors because the materials have an electronic energy state band gap at room temperature between their valence and conduction bands so that their intrinsic electrical conductivity decreases as the temperature is lowered.

ICPs are useful as chemical sensors because the electrical properties, typically the dc electrical resistance of these systems, are responsive to the presence of a diverse set of analytes in the vapor phase. Sorption of a vapor into an ICP will induce physical swelling of the material and will affect the electron density on the polymeric chains. The change in dc conductivity, $\Delta\sigma$, that results from sorption of an analyte can be divided conceptually into three components:

$$\Delta\sigma = (\Delta\sigma_c^{-1} + \Delta\sigma_h^{-1} + \Delta\sigma_i^{-1})^{-1} \qquad (5)$$

Here, $\Delta\sigma_c$ is the overall change in intrachain conductivity of the ICP, $\Delta\sigma_h$ is the change in intermolecular conduction due to electron hopping across polymer chains modulated by the presence of the analyte in the film, and $\Delta\sigma_i$ is the change in ionic conductivity between chains upon analyte sorption. The value of $\Delta\sigma_i$ is not only a function of the ion migration upon condensation of analyte but also is a function of proton tunneling rates if hydrogen bonding to the ICP backbone is significant.[85] These conductivity changes may, or may not, be linearly dependent on the concentration of analyte presented to the sensor, depending on the particular transduction mechanism involved in the ICP of concern.

The pathway for conduction through the conductive polymer backbone is more favorable energetically than across polymer backbones. Therefore, large changes in conductivity can be attributed to changes in the extrinsic conductivity of the material. For

example, highly oriented polyaniline is more conductive than amorphous polyaniline. Miller et al. have reported that a large increase in conductivity was observed upon exposure of a dinonylnaphthalenesulfonic acid doped polyaniline film to ethanol vapor.[86] Using both electron microscopy and wide-angle X-ray scattering, these workers were able to attribute this response to the crystallization of polyaniline. Hence, the hydrogen-bonding interactions between ethanol and polyaniline were sufficient to bring the polyaniline chains closer together, thereby decreasing the energy barrier for electron hopping and increasing the mobility of the charge carrier.

Intrinsically conducting polymers possess several potential advantageous features for use in sensor arrays for vapor detection. A diverse range of polymers is available via the electrochemical or chemical polymerization of a range of monomer types. The sensitivity of a sensor element can be readily altered by changing the polymerization conditions and the charge compensating counterion. The oxidation state of the polymer can be altered after deposition in order to tune the electronics of the polymer to be compatible with the analyte of interest such that an optimum charge transfer interaction may take place. Fabrication is easily performed through either electrochemical deposition and/or film casting from solution (for soluble analogues), which readily allows for miniaturization and mass production of sensors. Biomaterials such as enzymes, antibodies, and cells may be readily incorporated into such structures, and finally (but not exhaustively) reversible responses are typically obtained in relatively short time periods at ambient temperatures. Drawbacks are the relatively poorly understood signal transduction mechanism, high sensitivity to changes in humidity that necessitate operation in a controlled, conditioned, environment, and a relatively low diversity in affinity of the conducting polymers toward a very diverse set of analytes, thereby producing less than optimal separation of many analytes in the sensor array data space.

The response commonly reported for ICP sensors is the normalized change in resistance obtained from a two-probe resistance measurement, $(R_2 - R_1)/R_1$, where R_1 is the resistance before exposure to the analyte of interest and R_2 is the resistance of the sensor at steady-state conditions upon exposure to the analyte. The response has also been reported as either the change in resistance (2 probe) or the change in conductivity (4 probe).

ICPs have reached the commercial market as detectors in "electronic" noses (sensor arrays) sold by companies such as AromaScan,[87] Bloodhound,[88] AlphaMOS,[76] and Zellweger Analytics.[89] The AromaScan A32/50S Multisampler consists of an array of 32 conducting polymer detectors and is based on research initiated at the University of Manchester Institute of Science & Technology (UMIST) by Krishna Persaud. The Bloodhound BH114 consists of an array of conducting polymer and discotic liquid crystal detectors and is a product of research efforts at the University of Leeds. AlphaMOS has a commercial nose on the market that combines sensor technologies using arrays of conductive polymer resistive detectors, metal oxide semiconductor detectors, and TSM resonator detectors, each fulfilling a specific duty. The role of the conducting polymer array is to detect polar molecules, whereas the metal oxide semiconductor detectors are sensitive to nonpolar molecules and are insensitive to water. Finally, Zellweger Analytics, which purchased Neotronics in 1996, sells a portable version of its electronic nose for environmental monitoring applications.

B. Array Fabrication

Conductive polymer sensors are typically prepared electrochemically.[90−97] The electrodes are typically interdigitated electrodes or are a pair of metal leads separated by approximately 10−50 μm. The metal is typically Au and the substrate is an insulator, such as glass.[97]

The electrochemical deposition of ICPs is reasonably controllable because films can be electrodeposited onto metallized areas and the film thickness can be varied by monitoring the total charge passed during the deposition process. Polymers can be deposited using a number of different electrochemical waveforms, for example, potentiostatically, galvanostatically, cycled potential, or by pulsed potentiometry. The polymerization is usually carried out in a three-electrode configuration in which the working electrode is the sensor substrate. A positive oxidation potential is often applied to the working electrode that is sufficient to oxidize the monomer at which time the monomer undergoes oligomerization to a point at which the oligomers electroprecipitate onto the electrode surface. As the material grows it bridges the gap between interdigitated leads, thus making a simple resistor. Measurement of the total charge passed gives an approximation of the film thickness, and the final potential applied to the material will control the extent of doping. In addition to this technique, many conducting polymers substituted with pendant solubilizing groups are soluble in solvents that are normally employed for spin coating.[98−100]

Several strategies have been employed to create an array of ICP detectors with each detector having a different response toward a variety of analytes. First, many different single-ring heterocycles and multiring fused/unfused heterocycles readily undergo either electrochemical or chemical polymerization and can be used as ICP elements. Some of these include pyrrole, thiophene, aniline, indole, and carbazole. Second, each heterocycle can be substituted with a number of different side groups. Third, different counterions can be used to compensate the positive charge (for a p-doped polymer) generated upon oxidation of the ICP to produce the electrically conductive state of the polymer. Fourth, different oxidation states are attainable in each ICP and different polymerization conditions (i.e., by changing the oxidation potential, oxidant, temperature, solvent, electrolyte concentration, monomer concentration, etc.) can be used to generate a number of different sensors from the same monomer, because properties such as

Table 1. Twelve Conductive Polymers That Constitute an ICP Sensor Array That Were Prepared by Electrochemical Polymerization Using a Conventional 3-Electrode Electrochemical Cell[a]

sensor no.	polymer system	monomer concn (mol/dm^{-3})	electrolyte concn (mol dm^{-3})	solvent	growth potential (V)	final potential (V)	resistance (Ω)
1	PPy-BSA	Py 0.1	0.1	H_2O	0.85	0.00	1650
2	PPy-PSA	Py 0.1	0.1	H_2O	0.85	0.00	193
3	PPy-HxSA	Py 0.1	0.1	H_2O	0.85	0.00	27
4	PPy-HpSA	Py 0.1	0.1	H_2O	0.85	0.00	16
5	PPy-OSA	Py 0.1	0.1	H_2O	0.85	0.00	35
6	PPy-DSA	Py 0.1	0.1	H_2O	0.85	0.00	37
7	PPy-TSA (Na)	Py 0.1	0.1	H_2O	0.80	0.80	19
8	PPy-TSA (m)	Py 0.1	0.1	EtOH	1.20	0.00	70
9	PPy-TEATS	Py 0.1	0.1	H_2O	0.75	0.00	34
10	PPy-TEATS	Py 0.1	0.1	PC	1.10	0.00	37
11	PAN−$NaHSO_4$	AN 0.44	0.1	H_2O	0.90	0.90	44
12	P3MT-TEATFB	3MT 0.1	0.1	CH_3CN	1.65	1.65	13

[a] Reproduced from ref 101. The distance between gold electrodes was 15 μm. PPy is polypyrrole, BSA is butanesulfonic acid, HXSA is hexanesulfonic acid, HPSA is heptane sulfonic acid, OSA is octane sulfonic acid, DSA is decanesulfonic acid, TSA (Na) is *p*-toluenesulfonic acid sodium salt, TSA (m) is *p*-toluenesulfonic acid monohydrate, TEATs is tetraethylammonium toluenesulfonate, PAN is polyaniline, $NaHSO_4$ is sodium hydrogen sulfate, P3MT is poly(3-methylthiophene), TEATFB is tetraethylammonium tetrafluoroborate, Py is pyrrole, AN is aniline, 3MT is 3-methylthiophene, EtOH is ethanol, PC is propylene carbonate, and CH_3CN is acetonitrile.

morphology, molecular weight (conjugation length), connectivity of monomers, conductivity, band gap, etc., are dependent upon the polymerization conditions.

Polypyrrole is the predominant polymer in the Neotronics NOSE. Chemical variation is achieved by either changing the dopant ion or changing the polymerization conditions. The use of 12 different polypyrrole-based sensors produces classification between chemically similar samples over a wide range of analytes.[94] In a separate paper, Pearce et al. constructed a 12-element electronic nose.[101] Table 1 lists the 12 different sensors and the electrochemical conditions used to prepare them.

Ten of the elements consisted of polypyrrole prepared with different counterions and polymerization conditions while the eleventh and twelfth elements were a polyaniline and a poly(3-hexylthiophene) film, respectively. Hatfield et al. have reported the construction of a 20-element sensor array composed of derivatized polypyrroles, thiophenes and other heterocyclic polymers.[102] Serra et al. have reported the differences in sensitivities of various analytes to three different poly(3,3′-dipentoxy-2,2′-bithiophene) sensors.[103] Chemical variation in these films was achieved by performing the vapor phase polymerization of the monomer in the presence of different oxidizing salts. Serra et al. conclude that, under different oxidizing conditions, different sensors are prepared with sensitivities (percentage variation of the resistance) ranging from −6.22 to 1.77.

Jahnke et al. utilized an array of poly(2,5-furylene vinylene) sensors to construct an electronic nose[85] using a soluble precursor route involving an aldol addition reaction of 5-methylfuran-2-carbaldehyde with a basic catalyst to obtain the precursor poly(2,5-furylenehydroxyethylene). The polymers were then spin-coated onto the sensor substrate and thermally dehydrated to varying degrees, thus making different sensors by the amount of elimination that occurred. In a similar approach, De Wit et al. prepared an array of poly(2,5-thenylene vinylene) copolymer conductometric sensors.[98] Preparation involved making a sulfonium precursor polymer, dissolving this polymer in acetone, and spin casting it onto the substrate. Thermal elimination and chemical doping yielded the conductive PTV. The authors prepared both the unsubstituted PTV and a methoxy-substituted derivative. Thermal elimination to varying degrees created chemically different sensors in that the conjugation lengths of the conductive segments were different. Sensors were reported to exhibit an extreme baseline drift that rendered them inoperable after ca. 1 month, although they could be regenerated by redoping the polymers with iodine vapor. The responses were reported to be linear with concentration between 5% and 100% of the saturated vapor pressure for a series of nine test vapors (toluene, water, propanol, acetone, acetic acid, diethyl ether, ethyl acetate, methanol, and ethanol). In using both the relative response and the recovery time response, a single detector was able to distinguish between six of the nine analytes.

C. Applications

One of the more prevalent fields of application presented in the literature for the ICP electronic noses is monitoring the quality of foods and beverages.[104] A nose consisting of four different polythiophene sensor elements was used in conjunction with a taste sensor consisting of eight different polymer/lipid membranes. Using principal component analysis, four different wines were correctly identified and discrimination was successfully performed among five aged samples of the same wine. The authors concluded that sensor fusion of both the smell and taste sensor arrays led to enhanced discrimination.[99]

Numerous papers have been published on using the electronic nose to monitor the quality of beer.[101,105,106] In a detailed analysis performed by Pearce and Gardner, an array of 21 conducting polymers was used to predict organoleptic scores. In this study, a control lager beer was spiked with different reference compounds (diacetyl, dimethyl sulfide, and hop essence). For high concentrations of the reference compound in beer (>40 ppb), the

electronic nose performed worse than both gas chromatography and flavor profile analysis; whereas, at low concentrations, the accuracies were reported to be similar.[107]

The Aroma Scanner has been reported to be an efficient instrument which complements gas chromatography/mass spectrometry in the analysis of volatiles from both earth-almond and carob, which were both analyzed raw and roasted for different periods of time.[108] The correlation between the sensors and the GC/MS was reported to be 0.98 for earth-almond; whereas a lower correlation of 0.74 was obtained for carob. Schaller et al. reported that an electronic nose consisting of ICPs exhibited poor sensitivity to the volatile components of cheese with the main problem being attributed to sensor drift.[109] The Neotronics e-nose has been successfully applied to discriminate between different levels of boar taint.[110]

Many microorganisms are known to expel volatile chemicals. Work at the University of Leeds has led to both the detection and discrimination of 13 different types of microorganisms utilizing a 16-component sensor array.[111] Through use of a three layer perceptron network on data arising from 244 sample responses, a majority of the microorganisms were reported to be classified with a quoted success rate of 100%. Arnold et al. have investigated the use of an artificial nose to assess bacteria isolated from processed poultry.[112]

Conducting polymer-based electronic nose technology also has been reported to offer a rapid, reproducible, and objective method for sewage odor assessment.[113−116] In averaging all of the data from 10 different sewage treatment plants, the authors reported that at low concentration ranges (below 4000 odor units (ou)/m^3) the Neotronics eNOSE output correlated well with olfactometry data.[113] However, this was not the case at higher concentrations, due to saturation of the polypyrrole sensors. The data from a single sewage treatment plant exhibited a relationship between the electronic nose responses and the threshold odor number (TON) over a range of concentrations from 125 to 781 066 ou/m^3. Further work was carried out by Stuetz et al. using the eNOSE[114] in which canonical discriminant analysis was used to distinguish between different sewage samples from different treatment works. In this study, linear correlations were established between the electronic nose responses and the 5 day biochemical oxygen demand (BOD5) over time intervals of about 1 month. This array could be used for measuring chemical activity, making it a useful process control since it has been estimated that about 40% of the energy could be saved by using an on-line aeration control system. The e-NOSE has also been used to discriminate between untainted water samples and water tainted with geosmin, methylisoborneol, 2-chlorophenol, phenol, diesel, and 2-chloro-6-methylphenol.[115]

Researchers have utilized the electronic nose to monitor air quality in relation to the assessment of malodor in agriculture. Fresh liquid pig slurry was analyzed using GC/MS to identify the major components in the vapor phase. A 20-element ICP sensor array exhibited a linear response to methanol vapor, whereas nonlinear behavior was reported for acetic acid. Using Sammon mapping, each of the individual components and both basic and acidic pig slurry were discriminated.[117] Byun et al. have reported that the best way to visualize the data obtained from pig slurry is to combine both principal component analysis and Sammon mapping.[118] Furthermore, the AromaScanner has also been used to assess malodor concentration after the application of cattle slurry to grassland.[119] Masila et al. have demonstrated the usefulness of the Aroma Scanner to detect environmentally unfriendly halogenated organic compounds such as 2,4,5-trichlorophenol, pentachlorophenol, 1,1-bis(4-chlorophenyl)-2,2,2-trichloroethane (DDT), and 2,2-bis(4-chlorophenyl)-1,1-dichloroethylene (DDE), just to name a few. Using cluster and Euclidean distance analysis, both the identification and the quantification of these organic compounds were reported.[120]

The electronic nose has been successfully applied to several medical and veterinary science applications. To increase the likelihood of successful artificial insemination in cows it is beneficial to detect the occurrence of estrus. Lane et al. have been able to utilize the Neotronics eNose to associate odors with the estrus period.[121] For five Holstein-Friesian cows, both the luteal phase and the estrus phase were discriminated using principal components analysis.[121] The AromaScanner was used to identify the source of an off-odor from a pharmaceutical inhalant.[122] Furthermore, the AromaScanner was used to screen for bacterial vaginosis.[123] Following training of the nose to four positive and four negative cases, 16 of the 17 cases were recognized as being positive. Of the 43 negative cases, 33 were correctly identified as being negative. Thus, the positive predictive value of the test was calculated to be 61.5%.[123]

Recently, a conducting polymer sensor array has been used for monitoring the environment of a confined system. An artificial nose consisting of an array of 20 conducting polymer (UMIST) and 6 TSM resonators (HKR Sensor Systems) was utilized in the MIR-95 mission and was reactivated in the DARA-MIR 97 mission.[124] In this work, it was concluded that the artificial nose was useful in detecting a fluid leak of ethylene glycol in the cooling system, which ultimately led to contamination of the water supply. The sensor array was also was useful in monitoring the atmospheric quality after a small fire. Furthermore, it was reported that after 1.5 years in the MIR space station, the system showed little drift or degradation.[124]

D. Future Directions

Amrani et al. have carried out numerous studies investigating the use of impedance techniques to increase both the sensitivity and selectivity of ICP sensor arrays.[125−129] In this work, the authors report both the relative changes in resistance and the relative changes in reactance upon sweeping the measurement frequency for each sensor in a 20-element ICP array. Both the resistance and reactance

were reported to give a linear regression when the relative values versus the concentration of the analyte were plotted. The specificity of the array was enhanced when the dissipation factor as a function of frequency were plotted.[129]

The dissipation factor can be expressed as the ratio of the energy dissipated (purely resistive) per cycle divided by the energy stored (purely reactive) per cycle. Therefore, it was calculated as the ratio of the resistive part of the impedance divided by the reactive part of the impedance of the sensor. When the dissipation factor vs the applied frequency was plotted characteristic resonances were observed for a single sensor exposed to air, acetone, methanol, and ethyl acetate. Not only was excellent discrimination achieved but these resonances were claimed to be useful to identify components of mixtures of analytes.[129] Furthermore, in using alternating current (ac) techniques, sensitivity to a particular analyte was increased 18-fold. The authors noted that the impedance analyzer is not practical for real applications due to the time that it would take to make a high-resolution scan across a range of frequencies.[129] They suggested that a way to overcome this drawback would be to employ periodic signals containing many different frequencies such that all of the frequencies are presented to the sensor at once. Furthermore, it was suggested that Fourier transform techniques could be used to isolate the response of a sensor at any number of specific frequencies.[129]

V. Conductive Polymer Composite Chemiresistor Arrays

A. Theory

Electronic noses based on an array of polymer composite sensors have been developed using either carbon black[130] or polypyrrole[131] as a conductive filler and nonconductive organic polymers as the insulating matrix. The transduction mechanism for the polypyrrole composites is potentially quite complex in that the analyte can interact with both the insulating matrix and the conductive polymer; whereas the transduction mechanism of the carbon black composite sensors has been described on the basis of percolation theory. Upon exposure to an odorant, the composites will swell to varying degrees depending on the polymer−odorant interactions, and this swelling results in a change in the conductivity of the composite film. This response can be easily monitored using a conventional ohmmeter. Therefore, each sensor element in the array, consisting of a chemically unique insulating matrix, responds differently to a given odorant, resulting in a distinctive pattern. For example, carbon black composite sensor arrays consisting of 17 sensor elements can easily distinguish between a chemically diverse set of analytes and mixtures consisting of two chemically similar analytes.

Percolation theory[132,133] predicts that the resistivity, ρ, of a conducting composite will be given by

$$\rho = \frac{(z-2)\rho_c\rho_m}{A + B + [(A+B)^2 + 2(z-2)\rho_c\rho_m]^{1/2}} \quad (6)$$

where

$$A = \rho_c[-1 + (z/2)[1 - (\nu_c/f)]] \quad (7)$$

$$B = \rho_m[(z\nu_c/2f) - 1] \quad (8)$$

and where ρ_c is the resistivity of the conductive filler, ρ_m is the resistivity of the insulating matrix, ν_c is the volume fraction of the conductive filler in the composite, z is the coordination number of the conductive filler particles, and f is their total packing fraction ($\nu_c < f$). Since these sensors are believed to operate by this percolation conduction, it is possible to fabricate high gain sensors by working close to the percolation threshold, ν_p, which is given by $2f/z$, such that a small volume change would induce a large resistance change.

B. Fabrication

Sensor fabrication entails casting a thin film of the composite over two electrical leads. For polypyrrole-based sensors this was achieved by chemically polymerizing pyrrole using phosphomolybdic acid in a solution containing the insulating polymer. The solution was then used to dip coat the substrate, a cut 22 μF capacitor (interdigitated electrode pair with a lead separation of 15 μm).[131] Carbon black composite sensors were prepared simply by either dip coating an interdigitated electrode capacitor or by either dip coating or spin casting onto a glass substrate containing two gold leads separated by a 5 mm spacing.[130]

Lonergan et al. prepared a diverse carbon black-based conducting polymer composite sensor array consisting of 17 chemically different insulating polymers as listed in Table 2.[130] Responses were typically measured as the maximum relative differential resistance $(R_2 - R_1)/R_1$, where R_1 is the baseline resistance of the film prior to exposure and R_2 is the maximum resistance upon exposure to the analyte. Each of the analyte exposures produced an increase in the resistance of the sensor, which is consistent with percolation theory. However, this was not always the case with polypyrrole composite sensors, indicating a more complex transduction mechanism that involves both the swelling of the insulating matrix and/or the polypyrrole or specific electronic interactions of the analyte with the conducting polymer, which would change its intrinsic conductivity.[96]

The normalized, relative differential resistance data for a set of carbon black sensors produced a different pattern upon exposure to nine different analytes as would be expected by the chemical nature of both the insulating phase of the composite and the analyte. For instance, sensor 16 (poly(ethylene-*co*-vinyl acetate)/carbon black) is hydrophobic and thereby responds best to benzene, whereas sensor 6 (poly(N-vinylpyrrolidone)/carbon black) is hydrophilic and responds very well to methanol. Principal component

Table 2. Materials Employed in the Carbon Black-Based Conducting Polymer Composite Sensor Array As Seen in Ref 130

sensor no.	polymer	T_g[a]	T_m[b]	δ[c]
1	poly(4-vinyl phenol)			
2	poly(styrene-*co*-allyl alcohol), 5.7% hydroxyl			
3	poly(α-methylstyrene)	49		
4	poly(vinyl chloride-*co*-vinyl acetate), 10% vinyl acetate			
5	poly(vinyl acetate)	30		9.35
6	poly(*N*-vinylpyrrolidone)	175		
7	poly(carbonate bisphenol A)	150	267	
8	poly(styrene)	100	237.5	9.1
9	poly(styrene-*co*-maleic anhydride), 50% styrene			
10	poly(sulfone)	190		
11	poly(methyl methacrylate)	105		9.3
12	poly(methyl vinyl ether-*co*-maleic anhydride), 50% maleic anhydride			
13	poly(vinyl butyral)	51		
14	poly(vinylidene chloride-*co*-acrylonitrile), 80% vinylidene chloride			
15	poly(caprolactone)	−60	60	
16	poly(ethylene-*co*-vinyl acetate), 82% ethylene			
17	poly(ethylene oxide)	−67	65	9.9

[a] Glass transition temperature (°C). [b] Melting temperature (°C). [c] Solubility parameter $(cal/cm^3)^{1/2}$.

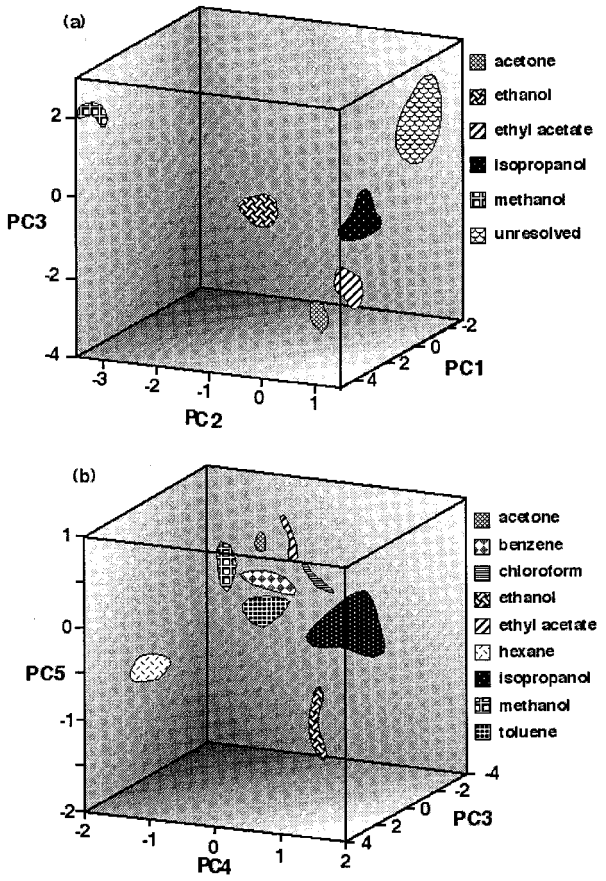

Figure 11. Results from the exposure of the 17-element array to nine solvents as represented in (a) the first three dimensions of principal component space and (b) the third, fourth, and fifth dimensions of principal component space. These five principal components contain over 98% of the total variance in the data. Reprinted from ref 130. Copyright 1996 American Chemical Society.

analysis was used to map the odorant patterns. The authors reported that the first five principal components contained greater than 98% of the total variance in the data. PCs 1−3 and 3−5 for the array are shown in Figure 11. This array distinguishes between a number of different classes of analytes and was able to distinguish between a homologous series of alcohols as shown in Figure 11 by the separation that was achieved for methanol, ethanol, and propanol vapors.

The carbon black-insulating polymer composite sensor array was exposed to a mixture of methanol and ethanol. The sensors in the array were found to give a linear plot of the response vs concentration for both of the pure components. Separate exposures to different compositions of the ethanol/methanol mixture yielded distinct pseudolinear paths between the responses of the pure component in principal component space. Therefore, the sensor array has demonstrated the potential to determine the absolute concentrations of a binary mixture.

One method used to increase the diversity of an array was to use compatible polymer blends as the insulating matrix.[134] A series of different sensors consisting of a poly(methyl methacrylate)/poly(vinyl acetate) blend in a number of different ratios and of both the pure polymers were studied. A plot of the detector response vs the mole fraction of poly(vinyl acetate) yielded nonlinear behavior for five different analytes. The compatible blend detectors clearly demonstrated an enhancement in maximizing the discrimination between analytes. Severin et al. have demonstrated that the incorporation of the chiral polymer poly((*R*)-3-hydroxybutyrate-*co*-(*R*)-3-hydroxyvalerate) into a carbon black composite detector allowed for the differentiation between enantiomeric odorants.[135] Doleman et al. have shown that the response intensity of a carbon black composite sensor is, to first order, determined by the thermodynamic activity effects that dictate the concentration of the analyte in the polymer matrix.[136] When the concentration of the analyte in the gas phase was maintained at a constant fraction of its vapor pressure, the mean response intensity taken as an average across a 13-element detector array remained constant for both a homologous series of *n*-alkanes and a homologous series of *n*-alcohols. This trend has been observed in human detection threshold judgments for the same homologous series of alkanes and alcohols.

C. Applications

Doleman et al. evaluated the performance tasks for three separate arrays of different conductometric sensors.[23] In this work they compared the resolving power of an array of intrinsically conducting polymers, an array of tin oxide detectors, and an array of carbon black conductive composite detectors by calculating the resolution factor according to the Fisher linear discriminant method for pairwise combinations of 19 different solvents. In general, it was shown that for all three sensor arrays that the array performance increased as the number of detectors increased. Furthermore, it was reported in their work that the carbon black−polymer composite detectors significantly outperformed the tin oxide and intrinsically conducting polymers arrays in resolving both the full set of 19 analytes and subsets thereof, as determined by the criteria of best resolving the analytes on average or best resolving the worst-resolved analyte pairs using the raw data responses.

One advantage to the use of detectors whose conductivities follow percolation theory is that their sensing properties can be controlled by changing the composition or loading of conductor in the insulating matrix. Having detectors that operate closer to the percolation threshold could, theoretically, lead to significant signal enhancement. The detection thresholds for carbon black detectors were initially estimated to be at 0.25 parts per billion.[130] Since it is more appropriate to report detection thresholds in terms of activity instead of concentration,[136] the detection thresholds have been measured to be 4×10^{-5} of an analyte's vapor pressure.[137] The concentration detection threshold data obtained both for a homologous series of alkanes with vapor pressures ranging from 5 to 100 Torr and a homologous series of alcohols with vapor pressures ranging from 2 to 100 Torr ranged from 0.1 to 100 ppm and from 0.1 to 1 ppm, respectively.

VI. Optical Vapor Sensing Arrays

A. Introduction

Optical sensors employ analyte-sensitive indicators for detecting chemical species. A multitude of transduction mechanisms may be utilized for detecting the analyte, including fluorescence intensity and lifetime, polarization, spectral shape, absorbance, wavelength, and reflectance. A typical optical sensor is composed of an optical fiber with an indicator immobilized on the fiber tip.[138] By immobilization of different polymer layers onto the fiber tip, the sensor can be tuned to distinguish between a particular analyte or a range of analytes. By combination of multiple fibers into an array format, such sensors can be designed to detect many analytes simultaneously. An optical cross-reactive array also employs multiple fiber sensors, but these sensors exhibit a broad, rather than a specific, response to different analytes. Several recent reviews describe these optical cross-reactive array systems.[139,140] While several other cross-reactive optical vapor sensing systems exist, they are not in an array format.[72,141−146] This section focuses on two formats of cross-reactive optical array: polymer-deposited fiber arrays and self-encoded bead arrays.

B. Polymer-Deposited Optical Sensor Arrays

Solvatochromic fluorescent dyes have been immobilized in various polymer layers to produce a sensor array for detecting organic vapors. The interaction between the immobilized sensing chemistry and the analyte generates local fluorescence signals that can be monitored over time.[147] One of the major advantages to using an optical approach for designing a cross reactive array sensor is the ability to collect many kinds of complex information simultaneously, including (but not limited to) changes in intensity, fluorescence lifetime, wavelength, and spectral shape. Increasing the dimensionality of a system, by observing many different parameters at one time, makes it possible to build a more sensitive, multianalyte detecting device with fewer sensors. A single solvatochromic dye (Nile Red) is immobilized within different polymer matrixes, each having its own baseline polarity.[148] Nile Red exhibits large shifts in its emission wavelength maximum with changes in local polarity. Typically, when exposed to solvents with increasing polarity, solvatochromic indicators will exhibit progressively more red-shifted absorption and/or emission spectra. The sorption of organic vapors into the polymer induces a change in the microenvironmental polarity, which is reported by the solvatochromic dye, as seen in Figure 12. By

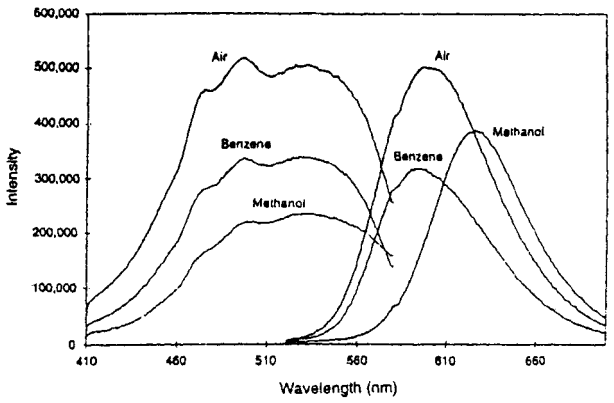

Figure 12. Fluorescence spectral changes of polymer-immobilized Nile Red with polarity changes imposed by different vapors (excitation on left, emission on right). Reprinted with permission from ref 150.

immobilization of the dye in polymer matrixes of varying polarity, hydrophobicity, pore size, flexibility, and swelling tendency, unique sensing regions are created that elicit different fluorescence responses when exposed to organic vapor pulses. The temporal response signals during these vapor pulses form the basis for unique patterns, which can then be used to train a computational network for subsequent analyte identification.

1. Array Fabrication

The distal ends of each fiber in the bundle are individually coated with different polymer/Nile Red combinations using either photopolymerization or dip-coating techniques. Photopolymerization involves

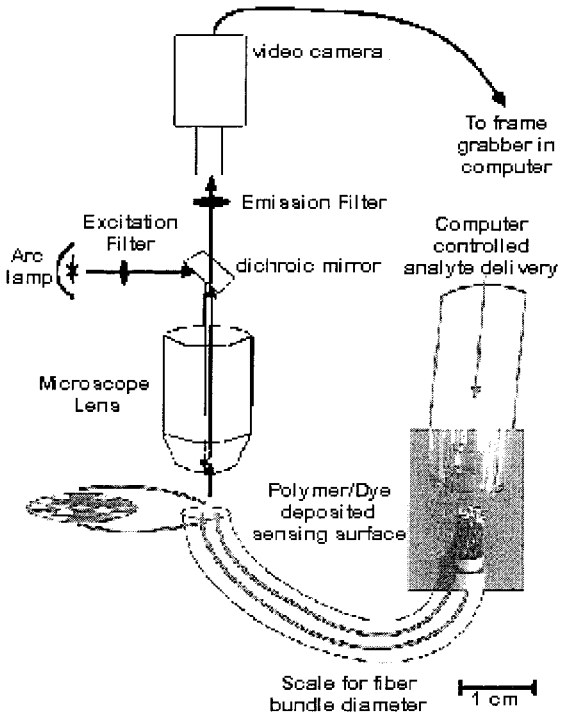

Figure 13. Schematic diagram of the video imaging and analyte delivery setup for the recording of responses of the optical fiber sensor array to applications of analytes. Reprinted from ref 151. Copyright 1996 American Chemical Society.

propagating ultraviolet light through the fiber to polymerize dye/monomer/initiator solutions onto the fiber tip. In the dip coating method, silanized fiber tips are repeatedly dipped in prepared Nile Red/polymer solutions and the solvent is allowed to evaporate between each dip. Both approaches result in Nile Red polymers attached to the fiber tips. Changing the amount of exposure to UV light or the number of solvent dips can alter the thickness of the polymer layers. Arrays can be assembled by bundling together multiple individual sensors with each sensor comprised of a different polymer. Alternatively, the entire array can be prepared on the ends of 350-μm-diameter fibers called image guides. Image guides consist of thousands of 3-μm optical fibers bundled together in a coherent fashion, such that each pixel's position is maintained from one end of the bundle to the other, allowing images to be transmitted down the length of the guide.[149] With these bundles one can photodeposit discrete polymer regions at selected positions on the face of the fiber using UV light, focused through a pinhole.

For detection, the proximal end of the fiber array is attached to a detection system comprised of a fluorescence microscope, light source, CCD camera, and computer. Filter wheels, shutters, and dichroic mirrors select and direct the appropriate wavelength of light used to analyze the optical arrays as shown in Figure 13. Vapor pulses are delivered through a vapor delivery system. Such pulses are analogous to a "sniff". Excitation light is introduced into the proximal end of the fiber and fluorescence from each sensor in the array returns through the fiber and is sent through an emission filter system and is then focused onto a CCD camera. The pattern of spectral

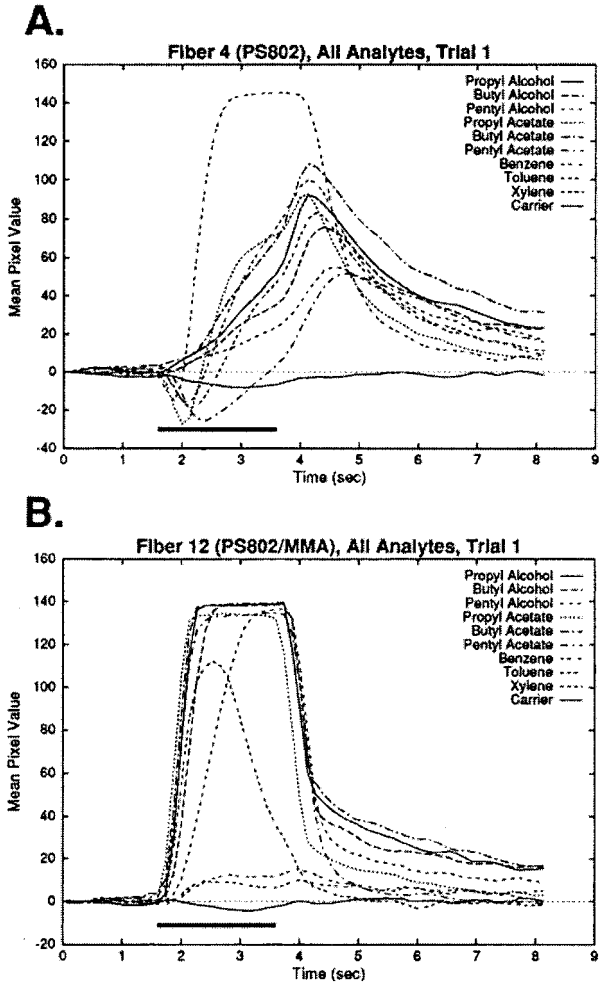

Figure 14. Examples of the responses of two different fibers (A, B) to all analytes presented as saturated vapor. The horizontal line at the bottom of each graph indicated the duration of analyte application. Reprinted from ref 151. Copyright 1996 American Chemical Society.

shifts exhibited by such an array upon exposure to different vapors is unique and characteristic for each vapor. These complex, time-dependent signals provide a "signature" for each vapor.[150−152]

The responses are monitored as a function of time versus mean pixel value (fluorescence). The fluorescence changes in these sensors are detected within milliseconds, and data are gathered by monitoring the fluorescence of each sensor in the array as pulses of different vapors are applied. As seen in Figure 14, two distinct responses are obtained when different vapors are pulsed onto two different polymer sensors. The time plots for fiber 4 demonstrate that the responses are distinct in their amplitudes and/or time courses for each analyte tested. On the other hand for fiber 12, the responses rapidly rise to a saturated plateau for five of the nine analytes tested.

2. Sensor Diversity

With the shift toward array formats comprised of large sets of cross-reactive sensors, a demand for new ways of creating diverse sensors has arisen throughout the sensor field. Polymerization reactions between different combinations of two starting materials lead to many new, different, nonlinearly related

sensing materials. This approach has been demonstrated in two ways: (a) the use of discrete polymer sensing cones each comprised of a specific monomer combination, (b) the fabrication of polymer gradient sensors. Gradient sensors were formed by scanning a pinhole-focused UV light beam across the proximal face of the fiber while steadily changing the concentrations of the two monomers in the solution being photopolymerized. The distal tip of the fiber resides, in the solutions, so that a polymer "stripe" forms as the photopolymerization occurs. The resulting polymer stripe contains all combinations of the starting and ending monomer concentrations. Responses from various regions of the gradient sensor were found to possess a far higher degree of diversity than did the corresponding region of a single component control stripe. In addition, responses from adjacent regions progressing down the length of the gradient stripe are not related to each other in a logical, linear fashion. One might expect different combinations of two monomers to yield sensors with responses that are simply related to the proportion of the two monomers used to construct the sensor. In actuality, such a progression is not observed: mixture responses do not appear to be linear combinations of the individual polymer responses. This individuality is most likely due to variation in polymerization kinetics and microstructure formation in the final polymer layer caused by the monomer ratio changes. In this way, it is possible to generate large collections of different sensing matrixes simply and efficiently from a limited set of starting materials.

C. Self-Encoded Bead Sensors

Decreasing the size of the sensor has enormous advantages in terms of both response time as well as the number of potential uses for such a device. Thousands of tiny beads (3.2 μm) can be immobilized in individual, acid-etched wells at the tip of an imaging fiber.[153] By introducing vapor-sensitive dyes into beads constructed from a wide range of polymeric and/or ceramic materials, it is possible to build an "ensemble" comprised of as many different types of sensor beads as necessary. Nile Red can be attached to different beads with the responses of all the beads from a particular preparation displaying nearly identical response behavior. Each bead class has a unique, well-defined response allowing individual beads to be easily identified after they have been deposited into wells. Since each bead type has its own unique response to a given vapor, the beads can easily be recognized *after* they have been placed into the image guide wells by simply exposing the array to a known test vapor and matching the resulting temporal response plots to those obtained beforehand for each bead class (Figure 15). In this way, the bead sensors are "self-encoding". The ability to prepare literally billions of identical beads in a single preparation should enable the computational network training to be transferred from one image guide ensemble to another.[154]

By using microspheres as sensor matrixes, the size of the overall array can be drastically reduced. This decrease in size in turn significantly shortens sensor response times while simultaneously enhancing sensor sensitivity. Silica bead sensors, for instance, were found to have response times on the order of ~150 ms, with signal changes of up to 1700%. On average, a 5-s experiment is ample time for most beads to fully respond to and recover from a pulse of vapor at any given concentration.

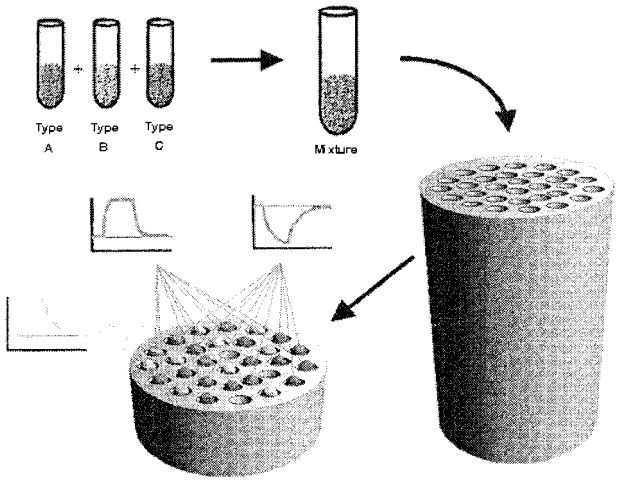

Figure 15. Schematic depiction of the self-encoded bead arrays concept. A mixture of sensor beads is prepared by combining aliquots from three stock solutions, each containing a different type of polymer/dye sensor suspended in a Nanopure water/0.01% Tween solution. A drop of the final mixture is then placed onto the distal tip of an etched imaging fiber. After they have settled in random locations throughout the well array, the beads are identified and categorized by their characteristic responses to a test vapor pulse, without the need for any additional encoding schemes. Reprinted from ref 154. Copyright 1999 American Chemical Society.

The recent development of an "electronic tongue", which is selective for the individual solutions, but not specific in their recognition properties, is an important step in the progress of optical cross-reactive sensor arrays.[155] Four taste categories, sweet, sour, salty, and bitter, were created from four different bead types, which measure combinations of pH, Ca^{+}, Ce^{+}, and simple sugars. Red, green, and blue light intensities were acquired for the each of the individual beads and used for the analyte quantification. The polymer response times were under 1 min, and the array was integrated allowing for continuous measurements of the bead−analyte response. The use of the red, green, and blue light intensities is a novel approach to sensor fabrication and provides a basis for combining an "artificial nose" with an "electric tongue" to gather both vapor and solution information.

D. Sensor Sensitivity

An important feature of any artificial nose is its ability to detect and quantify low concentrations of odors. In an effort to improve sensor sensitivity, common adsorbents have been incorporated directly into the sensing layers.[156] The most effective approach has been to directly adsorb dye molecules to the surface of alumina and silica particles. These particles are then adhered to fiber distal tips using various polymers and epoxies. The resulting sensors

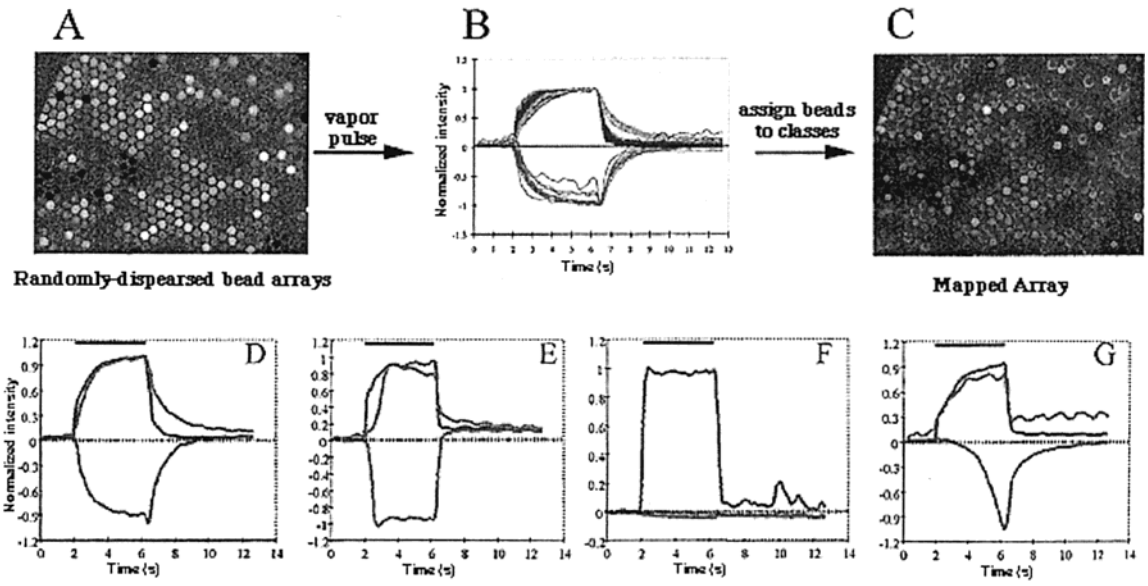

Figure 16. Data from a three-component self-encoded bead arrays (A). An initial pulse of methanol serves both as a vapor-sensing experiment and the array-decoding step. The three responses of the three bead types used are identified (B) to provide a map of the array (C). In this particular region are shown (D) methanol, (E) dichloromethane, (F) toluene, and (G) acetone. In D−G, traces represent the average response from each bead class. Reprinted from ref 154. Copyright 1999 American Chemical Society.

are capable of detecting vapors at much lower concentrations.

Another way to improve sensitivity is to sum the low-level responses of a large number of individual sensing elements (polymer beads), we have been able to produce large enhancements in the overall sensitivity of the array.[152,154] A similar approach has been used in the field of microelectrode arrays, where the advantages of microelectrodes (small size, rapid response times, small diffusion layers, and small *iR* drops) are combined with an array format in order to amplify the relatively small currents generated by individual microelectrodes. The primary difference, however, is that in the optical format, each element is individually addressable, making it possible to join the signals from large numbers of like elements randomly dispersed throughout the array. In addition, summing the responses from several beads at low vapor concentrations results in a substantial improvement in signal-to-noise ratios.

E. Data Processing for Optical Sensor Arrays

Pattern-recognition computational networks are used to analyze the data from the cross-reactive optical array sensors. The fluorescence changes are plotted versus time to produce a temporal response pattern for each sensing site for a particular vapor. The fluorescence response produces a series of characteristic patterns that are introduced as inputs to an neural network. Changes in fluorescence intensity data as a function of time contains sufficient information to accurately identify and quantify a broad range of organic vapors. In the first demonstration of the optical array's capabilities, a feed-forward neural network was able to correctly identify individual compounds, as well as components in binary mixtures, and to give a rough estimate of concentration.[150] In addition, the network was able to categorize compounds as aromatic, alcohol, or ester and to rank the relative molecular weights of compounds within a class. This latter capability seems to be due to the different response times of different analytes resulting from diffusion within the polymer layers. The sensor also has the ability to discriminate between vapors comprised of very similar functionality.[157]

In Figure 16, the data from an initial three-component system are described. Plotting the fluorescence intensity of the bead-containing wells with respect to time produces the characteristic response shapes. Methanol is used to decode the positions of the beads, as it provides a distinct response for the three bead types. Once the beads have been assigned, they are tested against three other vapors: dichloromethane, toluene, and acetone. Each vapor produces a distinct response to each sensor, and the combined use of the three sensors allows for the differentiation between the four saturated vapors. All of the resulting data are normalized to clarify the display and assist in the response−shape comparisons.

The self-encoded bead sensor array is an attractive approach because it can quickly accommodate new sensor bead types and is an improvement from the previous sensors in size, response and recovery times, ease of preparation, sensitivity, cost, and sensor reproducibility.

VII. Electrochemical Sensor Arrays

A. Introduction

In this section, we review multianalyte detection via cross-reactive electrochemical sensor arrays. By convention, most electrochemical array detection schemes incorporate identical and/or selective sensors that are not necessarily cross-reactive. These and

other array systems will only be discussed here if the sensor array was specifically designed to be cross-reactive in nature or if the cross-reactive responses from the sensor array are considered in the analysis.[158−174] Electrochemical arrays designed for the determination of one analyte,[175−178] multianalyte detection systems such as stripping voltammetry,[179−187] detection systems in which electrochemical sensor arrays are employed for chromatographic or electrophoresis separations,[188−200] or biosensor-related systems[201−203] will not be discussed. Individual sensors within a cross-reactive electrochemical array should show cross-sensitivity and/or cross-selectivity to multiple targets. As is the case for all the different cross-reactive arrays, it is also advantageous if individual sensors are sensitive or selective to varying degrees to target analytes so that different response patterns can be generated.

Over the last two decades, there has been a relaxed demand for highly selective sensors. More emphasis has been placed on sensor reproducibility, sensor stability, and the computational analysis software to retain the level of accuracy and/or detection limits for cross-reactive electrochemical sensor arrays.[158−163,166,169−174] Glass et al. has calculated that by incorporating a cross-reactive electrochemical sensor array in combination with a computational analysis program one can increase the amount of information content by at least 25% as compared to a single sensing element.[172] Thus, a cross-reactive array may supply the information necessary to predict target concentrations of multiple compounds in a known or an unknown matrix. As always, the information patterns generated by the sensor array are directly linked to the calibration techniques and experimental setup of the cross-reactive electrochemical array. There are also many variables which govern these response patterns, such as sensor material and size, solution or vapor composition, whether the reaction reaches equilibrium, and variation in sensor response, diffusion, and fluid dynamics (mixing, stirring, flow-injection, heat, etc.). There have been recent reviews in dynamic electrochemistry[204] and on chemical sensors[205] so many of these variables will not be discussed further, except where necessary.

B. Potentiometric (Equilibrium) Measurements

1. Principles of Operation

By definition, potentiometry refers to the difference in potential between two electrodes of a galvanic cell under the condition of zero current.[206] The indicator electrode is chosen so that it is responsive to the solution's target analyte and the reference electrode is invariant. This is an equilibrium measurement process because no current passes through the cell while the potential is measured. The potential of an electrochemical cell (E_{cell}) is

$$E_{cell} = E_{ind} - E_{ref} + E_{lj} \quad (9)$$

where E_{ind} and E_{ref} are the half-cell potentials for the indicator and reference electrodes, respectively, and E_{lj} is the potential at the electrode's liquid−junction interface. By employment of the Nernst equation, potentiometric measurements can provide accurate results for the concentration and activity coefficients of a target analyte. For example, in a general chemical reaction comprised of two half-cell redox reactions, $aA + bB \leftrightarrow cC + dD$, the Nernst equation would be

$$E_{cell} = E_{cell}^{\circ} - (RT/nF) \ln[(a_C^{\,c}\, a_D^{\,d})/(a_A^{\,a}\, a_B^{\,b})] \quad (10)$$

where E_{cell}° is the standard cell potential, R is the gas constant, T is the temperature, n is number of electrons involved in the reaction, F is the Faraday constant, and a is the activity of each chemical species. Many parameters affect the cell overpotential including temperature fluctuations, change of solution, electrode selectivity and sensitivity, and response to nontarget and interfering species in solution. Complexity in an electrochemical response is also related to adsorption of specific or nonspecific analytes on the electrodes and the nature of the electron transfer. Therefore employment of a "lock-and-key" sensor approach might only be feasible if the system is highly controlled. One may choose to control the temperature, employ solvents that minimize adsorption, or employ ion-selective electrodes (ISEs) to eliminate some of these variables. Theoretically, ISEs are "lock-and-key" sensors where each ISE is designed for one target ion. The ultimate goal, and biggest challenge in this field, is to build highly selective sensors that are not affected by interferents. However, nearly all ISEs developed to date have some cross-sensitivity (referred to as interferences) and respond in some fashion to other chemical species; herein lies the reason to employ these sensors in a cross-reactive array.

To discuss the use of ISEs in cross-reactive arrays, it is important to know how they generally operate and their original purpose. More background for this electroanalysis field can be found in a recent review.[207] ISEs are potentiometric sensors containing an ion-selective membrane that coats the electrode and sets up a potential due to transport of a single ion. The magnitude of this potential change is directly related to the specificity of the membrane for a target ion. A general schematic of an ISE is shown in Figure 17.

For an ISE, the potential of the membrane is considered and this changes eq 9 to

$$E_{cell} = E_{ref,ext} - E_{ref,int} + E_{mem} + E_{lj} \quad (11)$$

where $E_{ref,ext} - E_{ref,int}$ is the potential difference between the external and internal reference electrodes, respectively, and E_{mem} is the potential generated at the membrane. Usually the activity of the internal reference electrolyte is fixed and a plot of E_{cell} vs log(activity of analyte)[206] should be linear over the working range of the electrode according to eqs 12 and 14,

$$E_{mem} = (RT/zF) \ln[(a_i)_{samp}/(a_i)_{internal}] \quad (12)$$

where z is the charge on the ion and $(a_i)_{samp}$ and $(a_i)_{internal}$ are the potentials that develop on either side

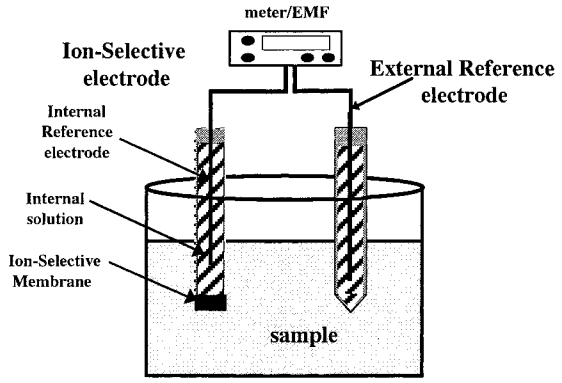

Figure 17. Basic schematic of an ion-selective electrode (ISE) used for potentiometric measurements. Upon interaction between the ion-selective membrane and the analyte, the potential across the membrane is altered. This potential change is dependent on the membrane specificity for a target ion in solution according to eq 11.

of the membrane for the target ion (i). For simplicity, the slope term (S) in eq 12 can be abbreviated

$$S = (RT/zF) \tag{13}$$

Assuming a fixed internal potential (a_i) and plugging E_{mem} into eq 11 produces the potential of the electrochemical cell as

$$E_{cell} = E_{ref,ext} - E_{ref,int} + (S)\ln[(a_i)_{samp}] + E_{lj} \tag{14}$$

The terms $E_{ref,\,ext} - E_{ref,\,int}$ and E_{lj} are constant so the only variables in the system are the target (i) ion activity and/or slope variation. These systems can still suffer from nontarget selectivities, interferents, and species buildup on the membrane. Therefore, ISEs find common application in solutions where there are low levels of interfering ions or where the concentrations are fixed to match those of calibration samples *unless* an ISE's cross-selectivity is used as an advantage. Many ISEs may be employed in the same sensor array. If each ISE within the array has varying degrees of selectivity/sensitivity for target analytes, this cross-reactivity can be an advantage and response patterns for each sensor can then be used to train a system for target determination. An array of ISEs may be used for multianalyte detection schemes as long as some type of computational analysis is employed. After modeling of an array of ISEs, the observed potential in the solution of unknown composition can be decoupled into those contributions arising from the target analytes and those arising from the interferents. This can improve precision when linked to an analysis scheme. The push to develop more sophisticated and intelligent systems involves acquiring the total analytical signal for accurate determination of the individual components. However, the acquisition of redundant (and nonuseful) information for such arrays does not benefit a system's prediction ability. Therefore, employing a variety of differentially responsive electrochemical sensors into an array and monitoring each sensor's response to a given analyte or analyte mixture will generate more useful information for target determination.

2. Examples of Potentiometric Arrays

As briefly stated above, ISEs are often unintentionally cross-reactive in nature because binding interactions between the membrane and nontarget chemical species. In this review, ISE array-types are not considered cross-reactive unless each electrode's nontarget responses and/or cross-selectivity are examined and/or incorporated into the analysis. For example, ISE arrays employing more than one type of sensor-element may be suited for multianalyte detection[208,209] but if sensor cross-selectivity is not considered or factored into the analysis these will not be discussed.

The membrane of the ISE will directly determine that sensor element's degree of cross-selectivity. Systems can be designed to be cross-reactive according to known membrane−analyte interactions.[207] For an ISE array to be considered cross-reactive, it must incorporate two or more ISE-types, be employed to determine more than one analyte, and use the electrochemical responses from many or all species in solution. Some groups have employed arrays of semiselective or sparingly selective electrodes in their cross-reactive arrays.[158−160] Sparingly selective electrodes are nonspecific ISEs and have been used for the specific purpose of generating more cross-reactivity within a sensor array because they respond to many analytes in varying degrees of selectivity. Otto and Thomas[158] may have been the first to perform these types of experiments in which nonspecific ISEs were employed in combination with a chemometrics program to identify concentrations of multiple targets within a mixture. They report on the simultaneous determination of free metal ions (Ca^{2+}, Mg^{2+}, K^+, Na^+) at physiological concentration levels. Such response data cause eq 14 to be transformed into a much more complicated system for each electrode−analyte response and can be thought of as an extended Nernst (Nicholski) equation

$$E_{ij} = E_j^\circ + S_j \ln(a_{ik} + \sum_l K_{jk} a_{il}) \tag{15}$$

These notations are employed in Beebe et al.'s[159] work where E_{ij} is the potential of the jth electrode, measured in the ith sample with respect to the reference electrode. E_j° is the intercept potential when the analyte activity a_{ik} is 1 M and the interferent levels, a_{il}, for all l interfering ions, are zero; K_{jk} is the selectivity coefficient of the jth electrode for kth ion, and S_j is the measured slope of the electrode in the absence of interferents. In the unique case where an ISE is not cross-reactive or there is no cross-selectivity toward nontarget ions, a selectivity coefficient for all lth ions would be zero, essentially eliminating the summation factor in eq 15. A more complicated version of this equation would be needed if ions of mixed valences affected the membrane potential, as suggested in eq 12. However, Otto and Thomas[158] found that they could use the valence (z) of the ion (i) regardless of the valences of the lth interfering ions. The most difficult problem that they encountered was the direct identification of Mg^{2+} in the presence of Ca^{2+} because the Mg^{2+} ISE

Table 3. Prediction of Remaining Nine Samples[a]

	predicted concns (% error)	
sample *i*	$[Na^+]$, M	$[K^+]$, mM
2	0.1198 (0.2)	3.73 (2.4)
4	0.1198 (0.1)	6.86 (2.0)
7	0.1351 (0.1)	3.89 (1.8)
9	0.1349 (0.1)	7.15 (2.1)
11	0.1498 (0.1)	2.03 (1.5)
14	0.1497 (0.1)	7.00 (0.0)
15	0.1486 (0.9)	8.45 (0.6)
17	0.1665 (0.9)	3.69 (3.4)
19	0.1641 (0.5)	7.03 (0.4)

[a] Reproduced from ref 159. Copyright 1993 American Chemical Society.

lacked selectivity for magnesium over that of calcium. They overcame this difficulty by employing more ISEs than they had targets, i.e., an overdetermined system, in combination with multiple regression analysis based on partial least squares (PLS). In a four component solution which simulated concentration levels in bodily fluids (blood serum or urine), they were still able to determine Mg^{2+} in the presence of Ca^{2+} using the responses from the cross-reactive array. Incorporating more sensors than they had target analytes, i.e., eight sensors, and incorporating PLS analysis, the prediction errors were approximately 4.5% (Ca^{2+}), 6.8% (Mg^{2+}), 2.3% (Na^+), and 1.4% (K^+).

Otto and Thomas[158] based their measurements on E_j° and K_{jk} and calibrated their sensors with knowledge of their slopes, as opposed to the work by Beebe et al.[159] who extended this work to see if they could calibrate an array of sensors without prior knowledge of sensor slope. Otto and Thomas[158] noted that multivariate calibration for the ISE array is hindered by the need to employ a constant overall ionic strength of the solution (fixed boundary conditions) while simultaneously varying the concentrations for each ion-type. However, they also used calibration solutions that did not contain interferents that may have caused some problems when moving to test solutions. Any errors associated with the calibration would also be incorporated into the test set. Beebe et al.[159] avoided these methods by varying the Nernstian slopes which led to an advantage in the calibration process where less error was predicted in the test set. They employed five to eight nonspecific ISEs in their cross-reactive array, and without having any potassium-selective sensors, they detected K^+ (2−10 mM) in the presence of much higher Na^+ levels (135−155 mM) in the matrix. According to their calibration methods, their use of only sparingly selective electrodes, and their analysis scheme, they attained lower prediction errors than Otto and Thomas;[158] however, unlike Otto and Thomas, they did not employ ions of mixed valences. Table 3 shows the results of Beebe et al.'s study.

This experiment demonstrated the feasibility of using a nonspecific sensor array to determine ion concentrations with reasonable accuracy. Beebe et al. went on to analyze their data to see if *each* of the five employed electrodes could be used alone to predict sodium concentration levels when potassium ions were ignored. For the single-sensor system(s), the prediction errors for nine samples varied between 0 and 38%, further emphasizing the benefit of cross-reactive electrochemical arrays and the increase in information content for analyte detection. Beebe and Kowalski[160] then attempted to expand this work by calibrating their cross-reactive array without a priori information about the functional relations between the responses and the ion concentrations. Unlike previous work[158,159] they did not base their calibration models on the assumption that the electrodes obey a certain equation. They merely used their array of nonspecific ISEs to prove their algorithms had the ability to determine binary mixtures of Na^+ (0.120−0.165 M) and K^+ (2.0−8.4 mM) in aqueous solution with average prediction errors lower than 5.3%.

Forster et al.[162] employed three highly specific ISEs in combination with one sparingly selective electrode in their cross-reactive array for determining sodium, potassium, and calcium ions in tertiary mixtures. They used this overdetermined system to poll results which enhanced the amount of information gained through cross-talk between sensors without introducing significant error from unmodeled interferents. It should be noted that although they employed three highly specific ISEs, the determined selectivity coefficients for the sodium, potassium, and sparingly selective electrodes suggested that these electrodes were not as selective as the calcium electrode (note different valence) in the presence of interferents. By incorporation of the sparingly selective electrode with the 3 selective sensor elements into an array, their prediction errors for 12 samples were improved from 4.5% to 2.8%, relative to the prediction errors for the 3 selective-element array alone. The array was able to determine each ion in a high interference background when the solutions did not contain unmodeled interferents. Forster and Diamond[163] used the same cross-reactive array model and analyte targets in combination with flow injection to improve prediction performance for mineral water and human plasma samples. They attributed the results to the kinetic factors (not equilibrium) associated with the flow injection sample delivery. Their array showed enhanced sensitivity for the target ions and they were able to determine these ions, without worrying about responses from unmodeled ion interferents such as Mg^{2+}.

In a related model, Diamond and Forster[164] employed three specific ISEs (for Na^+, K^+, Ca^{2+}) with a multiple ionophore electrode. They tailored the fourth electrode's selectivity by incorporating an ionophore for each of the target ions into the membrane. This array system, though more specifically designed, meets the cross-reactive array criteria. The array was more responsive to the three target ions relative to the multiple ionophore electrode as seen in previous work[163] with a sparingly selective electrode. However, even though this array was cross-reactive, the calibration and tests were specific for particular defined reaction conditions and could not be implemented into unknown systems. Finally, Legin et al.[165] used an array of electrodes to detect zinc ions in a background with three other metals (Cu^{2+}, Pb^{2+}, Cd^{2+}) even though there was no zinc-selective elec-

trode employed. The sensors were incorporated into an array, and the system was trained on complex solutions of heavy metals (Cu^{2+}, Pb^{2+}, Cd^{2+}, Zn^{2+}, Cl^-, F^-, and SO_4^{2-}) in concentration ranges typical of industrial waste. All the species were identified even without having specific sensors for each of the target analytes, i.e., zinc and sulfate.

C. Voltammetric (Nonequilibrium) Measurements

1. Principles of Operation

In contrast to potentiometry, where there is no applied current, voltammetry is the measurement of the current−potential relationship in an electrochemical cell where equilibrium is not established. There are many voltammetric methods: square wave, staircase, pulse and differential pulse, cyclic, anodic stripping, and amperometric titrations. Again, we will only deal with those areas that employ cross-reactive sensor arrays. In voltammetric measurements, information about a target analyte is generated from the measurement of the current as a function of the applied potential under conditions, which enhance polarization of the working electrode.[210] The reference electrode's potential is constant, and the working electrode assumes the value of the applied potential. Therefore, the working electrode is the site where electrolysis occurs and this generates the measured current. The current is quantitatively related to the speed of the electrolytic process, which in its simplest form, is a redox half-cell reaction:

$$M^{n+} + e^- \leftrightarrow M^{(n-1)+} \qquad (16)$$

Here M^{n+} is the electroactive species which is reduced to $M^{(n-1)+}$ (or the reverse reaction where $M^{(n-1)+}$ is the electroactive species oxidized to M^{n+}). Sensors based on detecting the current flow caused by oxidizing or reducing an analyte are highly successful because of their selectivity and high sensitivity coupled to the wide range of organic and inorganic analytes that can be detected using this technique.[211] If one were to employ an array of working electrodes, each element *could* generate an independent measurement signal. An important feature of many voltammetric-type arrays is the movement toward miniaturization. Arrays of microelectrodes used in voltammetry can have either *all* the electrodes interconnected to produce one overall measured current, or *each* of the electrodes can have different applied voltages and allow individual electrodes to register a current. These arrays can also offer significant improvements in sensitivity, *S*/*N* ratios, and detection limits so combining these advantages into a cross-reactive array with an incorporated computational analysis program can lead to highly effective and intelligent detection systems. One can use the time response or even use different potentials for different sensors to generate more information that can be used for target discrimination. Considerable effort has been applied to controlling the reactivity of amperometric sensors by modifying the surfaces with thin films, metal layers, polymers, or biological materials. Therefore, cross-reactive voltammetric arrays can be generated by employing different potentials to the individual elements, employing an array of different electrode types, modifying the electrodes, or using a combination of these approaches.

2. Examples of Voltammetric Arrays

An array of cross-reactive amperometric sensors was employed by Stetter et al.[166] to detect 22 organic vapors (20−300 ppm) in a portable system. This system consisted of four uncoated electrodes, each operating at a different potential and preceded by different filament catalysts to pretreat the incoming vapor flow before presentation to the array. The four sensors with their applied potentials were the following: (a) Au, −200 mV; (b) Au, +300 mV; (c) Pt, +200 mV; (d) Pt black, 0 mV. As noted, the sensors were set at different oxidation and reduction potentials and the four modes used to acquire data were the following: (1) no filament used; (2) platinum filament at fixed temperature; (3) rhodium filament at fixed temperature; (4) rhodium filament at a second fixed temperature. The heated filaments can partially oxidize some of the vapors as they flow to the amperometric sensors. In all, 16 separate channels of information were generated for each of the chemical species in the test set. Many of these data channels contained unique information that was analyzed with pattern recognition software.

One goal of Stetter et al.'s work was to detect and discriminate the vapors in the test set and minimize the number of sensors employed. The amperometric sensors used were known to fluctuate by as much as ±25% over the course of 1 month so they incorporated ±25% random noise into the response patterns to see how their prediction errors varied. When they removed redundant data and incorporated nonlinear mapping to check the original data set in combination with two sets containing random errors, only two analyte vapor pairs overlapped in the cluster analysis (nitrobenzene/acetone; cyclohexane/acetic acid).

Though more sensors need to be incorporated for better discrimination, these results show that by employing a four-element cross-reactive amperometric array, nearly 22 vapors could be discriminated and detected at ranges between 20 and 300 ppm using pattern recognition analysis even when ±25% random error was incorporated into the array. In a related study with the same array model and pattern recognition, Stetter et al.[169] classified grain quality according to patterns for "good", "sour", or "insect" wheat classes with good accuracy. In another similar approach, Schweizer-Berberich et al.[170] characterized fish freshness vs time with an eight-element cross-reactive array employing a filament catalyst varied over five temperatures. Forty channels of data were generated, and principal component analysis (PCA) and principal component regression (PCR) were used for data analysis.

Using the same four-element array model, Stetter et al.[167] aimed to use only *one* sensor's response from the array to perform analysis. In the defined system, it was determined that sufficient information was generated from the one-sensor/one-filament in order

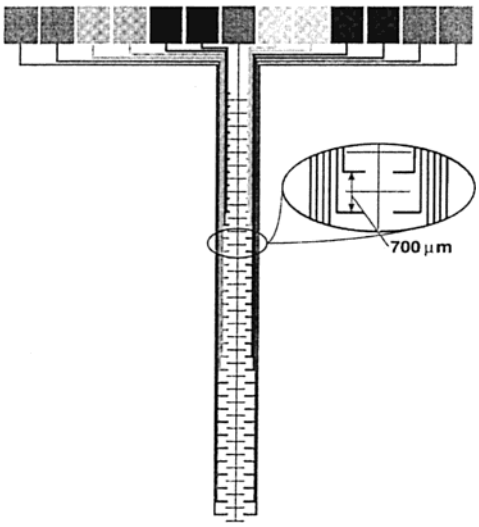

Figure 18. Diagram of a microelectrode array. The insert shows spacing between working electrodes. Electrical contacts are made at the top of the chips, and there are two pads for each shown electrode. From left to right (pad numbers): Pt (1,2), carbon (3,4), V (5,6), Pt auxiliary (7), Au (8,9), Ir (10,11), and Pt (12,13). For each material, one contact pad leads to a single electrode and the other pad leads to an array of 10 electrically connected together. There are 66 working electrodes, and the platinum auxiliary electrode runs down the center. Reprinted from ref 172. Copyright 1990 American Chemical Society.

to quantify and identify certain compounds and mixtures. In a related study, Vaihinger et al.[168] reasoned that one electrochemical sensor in combination with one catalytic filament could be employed to identify and quantify pure gases and mixtures by varying filament temperatures. Although this single-element system is not an array, the multiple information obtained from the sensor serves to increase the dimensionality of the data and thereby enables the sensor to improve its ability to solve analytical tasks. In a relatively similar effort as Stetter et al.[167] and Vaihinger et al.,[168] Glass et al.[172] tried to compare the amount of useful information one sensor element could generate as compared to a five-element cross-reactive array. The microelectrode arrays were produced by photolithography and employed two sensors for each of the five different sensor types (Figure 18).

For one electrode (Pt), they compared data at five different potentials (−0.2, −0.5, −0.8, −1.0, and −1.2 V) vs the data at one potential (−1.2 V) across the five-element electrode pairs. These data did not provide identification of analytes; however they show that the average information content gained for the cross-reactive array relative to one sensor element was 25%.

Wang et al.[171] took a different approach to creating sensor diversity for developing a cross-reactive sensor array. The four amperometric sensors were each coated with a different semiselective film of varying pore size, charge, and polarity, and unlike Stetter et al.,[166] all the sensors within the array were maintained at the same potential. They used this array as a thin film detector to quantify neurologically significant catechol compounds such as dopamine, (3,4-dihydroxyphenyl)acetic acid (DOPAC), epinephrine, norepinephrine, and catechol using flow injection to deliver the sample to the array. See Figure 19 for the array schematic.

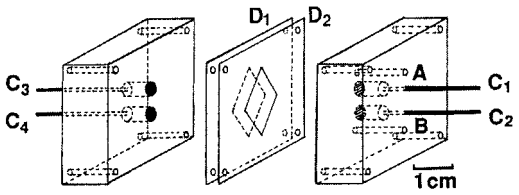

Figure 19. Enclosed view of the thin-layer flow cell: (A, B) solution inlet and outlet; (C_1−C_4) working electrodes; (D_1, D_2) spacers. Reprinted from ref 171. Copyright 1990 American Chemical Society.

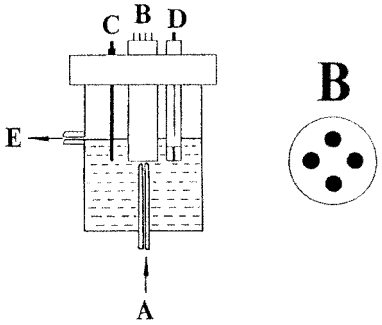

Figure 20. Schematic view of the large-volume wall-jet detector: (A) inlet; (B) electrode array; (C) counter electrode; (D) reference electrode; (E) outlet. To the right is the bottom view of the electrode array (B). Reprinted from ref 173. Copyright 1993 American Chemical Society.

Wang et al.'s array exhibits unique responses to the analytes because of partial selectivity and employs multiple linear regression analysis. Sensor diversity is directly related to the film employed and produced different current responses over time when all the sensors were held at the same potential. For instance, the smaller catechol compounds transport readily through the size-exclusion cellulose acetate layer to produce larger sensor responses than dopamine. In other data not shown, Wang et al. also used this cross-reactive array and applied different potentials to the four elements and showed that a third dimension can be used to generate more information for better analyte determination.

Chen, Wang, and co-workers[173] modified the electrode elements to create even more sensor diversity. They modified four carbon paste electrodes with metal oxide catalysts (Cu_2O, RuO_2, NiO, and CoO) and kept all the elements at the same potential to determine individual carbohydrates and amino acids in different sample mixtures by amperometric flow injection. Figure 20 is a schematic of the array system. Each modifier shows a different electrocatalytic behavior toward each analyte. Figure 21A (carbohydrates) and Figure 21B (amino acids) show the generated response patterns for the sensor array, i.e., the analyte fingerprint.

The distinct electrocatalytic properties for each sensor results in unique responses for the analytes when tested within the dynamic range of the sensor array. Using statistical regression analysis with two and three component mixtures, the prediction errors for analyte identification ranged from 0 to 11%, whereas the average value was 2.3% for the sensor array. Like Wang et al.[171] they show that more

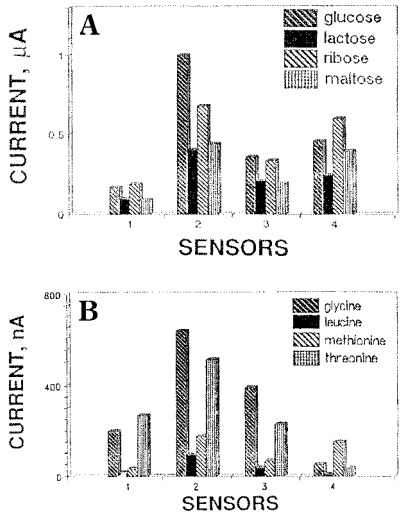

Figure 21. Sensor response patterns for the listed carbohydrates (A) and amino acids (B). The carbon paste electrodes are modified with the following metal oxides: (1) CoO; (2); Cu_2O (3) NiO; (4) RuO_2. Reprinted from ref 173. Copyright 1993 American Chemical Society.

information can be extracted when multiple potentials are applied to the individual sensor elements. In a recent publication, Amatore et al.[212] employed paired-band microelectrode assemblies to mimic physiological neuronal processing to observe current vs time relationships for two species using square pulse voltammetry. Their system offers many advantages for use in cross-reactive arrays because of on-line logic processing and the degree to which sensor variations could produce diversity in the system's response profiles. In a final related voltammetric approach, Wehrens and van der Linden[174] examined calibration data from an array of individually modified electrodes to determine the best analysis protocol for nonlinear voltammogram data from four chemically similar compounds. Different voltammograms were expected for this array because they used modified electrodes. Sixteen Ir electrodes were employed, six of which were modified with Au (2), Rh (2), and Pt (2), and they used PCR analysis for the calibration data and artificial neural networks to determine the best tool for analysis. They state that it is possible to use such an array to quantify multiple components in a sample although their results were not that convincing.

VIII. Acoustic Wave Devices

A. Introduction

Piezoelectric materials produce a voltage when mechanical stress is applied, and conversely will deform if a voltage is applied across them. When an oscillating potential is applied at a frequency near the resonant frequency of a piezoelectric crystal, a stable oscillating circuit is formed. Depending upon the geometry of the crystal and electrodes, a variety of wave modes can be established.[213] Two device types have been used to construct electronic noses: thickness-shear mode (TSM, also called quartz crystal microbalance (QCM) and bulk acoustic wave (BAW)) and surface acoustic wave (SAW) resonators. These

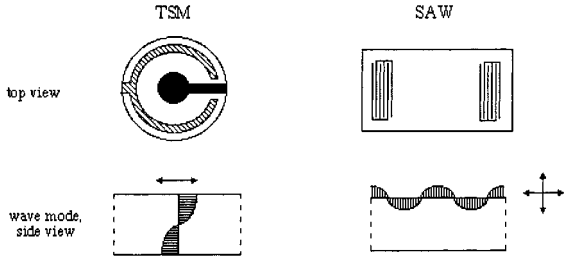

Figure 22. Thickness-shear mode (TSM) and surface acoustic wave (SAW) resonators. On top are shown the quartz crystals and their gold contacts (on two sides of the crystal for the TSM). On the bottom are schematics of the wave that propagates in each resonator.

devices are commonly constructed from quartz crystals, with the configurations shown in Figure 22. In a TSM resonator, the acoustic wave propagates through the bulk of the crystal in a direction perpendicular to the surface, with motion at the surface parallel to the surface. In a SAW device, motion occurs only at the surface, penetrating to a depth of approximately one acoustic wavelength into the crystal. The direction of propagation is parallel to the surface, while motion at the surface is both parallel and perpendicular to the surface. SAW devices can be constructed in two different configurations, delay-line and resonator, as pictured in Figure 22. TSM devices typically operate at frequencies from 5 to 30 MHz, while SAW devices generally operate between 100 and 400 MHz.

Adding mass to the surface of acoustic resonators changes their resonant frequency, and Sauerbrey derived eq 17 to describe the frequency shift of a

$$\mathrm{d}F = 2.3 \times 10^6 \times F^2(dM/A) \qquad (17)$$

quartz TSM resonator resulting from a change in mass on its surface.[214] The change in frequency (dF) is proportional to the original frequency squared and the change in mass per area of the crystal surface. A resonator coated with a material, such as a polymer, that absorbs organic molecules from the gas phase would be expected to change its resonant frequency upon exposure to organic vapors. The Sauerbrey equation is of course an approximation that is valid under certain conditions; for relatively thick films of hard polymers, sorption-induced changes in viscoelastic effects can also contribute to the observed frequency shift. King first utilized quartz TSM devices coated with common GC stationary phases as a detector of organic molecules exiting a GC column.[215] Wohltjen and Dessey were the first to use coated SAW resonators to detect organic vapors.[216]

B. TSM Arrays

In 1986, Kowalski and co-workers first examined arrays of polymer-coated TSM resonators.[217,218] Their data[219] consisted of the responses of 27 coatings on TSM devices exposed to 14 different analytes. Principal components analysis (PCA) was used to analyze the matrix of responses and indicated that 95% of the variance in the data was present in the first 7 principal components. The authors concluded that an

array of seven sensors comprised of those with the greatest contribution to each of the first seven PCs would represent a near-optimal array.[217] The same data set was analyzed to determine what subset of sensors could provide the best sensitivity, selectivity, signal-to-noise ratio, and limit of detection. Since the original data consisted of only one response for each sensor−analyte pair, an estimated random noise was added to the data. One seven-sensor array consisted of the most sensitive individual sensors, while a second array consisted of seven sensors chosen using PCA as outlined above. A set of equations developed by Lorber[220] that describe the sensitivity and selectivity of an array of partially selective sensors to particular analytes was used to compare the two sensor arrays. It was found that while the two arrays had similar overall selectivities, the PCA-selected array was substantially more sensitive to all the analytes tested. For one sensor, a detection limit can be defined, commonly at the analyte concentration at which the signal-to-noise ratio is three. For an array of sensors, an analogous *limit of determination* (LOD) can be defined for an analyte in the presence of other possible interfering components. The LOD for a variety of analytes were generally lower for the PCA-selected array of sensors. A comparison of the determined case (seven sensors, seven analytes) and the overdetermined case (seven sensors, three analytes) shows that in the overdetermined case the LOD decreased by nearly 2 orders of magnitude.

Kowalski and co-workers constructed a nine-sensor array and determined the concentration of individual analytes in two- and three-component mixtures.[221] The methods of multiple linear regression (MLR)[222] and partial least squares (PLS)[223] were used. For the two-component mixtures, PLS predicted concentrations approximately 5 times better than MLR did. The relative prediction error of PLS for two-component mixtures was 4.6%, while individual sensors have a 3−6% relative response error. For the three-component case, the average PLS prediction error was 10.1%, while that of MLR was 18.6%. Carey and Kowalski used a similar six-sensor array to monitor the solvent vapors exiting an industrial process dryer simulator.[224] Principal component regression (PCR) was used to calculate the concentrations of vapors exiting the chamber, and the values agree with those that would be expected.

Göpel and co-workers first investigated arrays of TSM resonators coated with both polymer and nonpolymer materials in 1991.[225] A variety of functionalized polysiloxanes on TSM resonators were exposed to a series of organic molecules, and the strengths of their various interactions were discussed.[226,227] A correlation was noted between log K (K is the polymer−gas partition coefficient) and T_b/T' (T_b is the solvent's boiling point, and T' is the temperature at which the measurements are made). After the boiling point correlation was corrected for, the expected trends were observed: relatively nonpolar organic molecules were absorbed strongly by poly(dimethylsiloxane), polar organic molecules were most strongly absorbed by poly(cyanopropylmethylsiloxane), and polarizable molecules were relatively well absorbed by polyphenylmethylsiloxane. Cellulose derivatives were also used as coating materials.[228] Both PLS and artificial neural networks (ANN) were tested for their ability to predict concentrations of analytes in mixtures, and ANN were found to slightly outperform PLS.[229,230] Neural networks were also used to dynamically monitor an analyte stream.[231] An array of TSM devices coated with siloxane polymer, metal complex-modified siloxane polymer, or pure metal complex was used to sense organic vapors and was found to be particularly sensitive to oxygen- and nitrogen-containing molecules.[232] A hybrid array containing polymer-coated TSM resonators, tin oxide gas sensors, electrochemical sensors, and metal oxide semiconductor field effect transistors (MOSFETs) was used to discriminate coffees, olive oils, tobaccos, and whiskeys.[51] Chiral GC stationary phases that consist of polysiloxanes with chiral side chains were coated on TSM resonators, and small arrays of these devices were used to discriminate enantiomeric odorants.[233,234] In another study, the coating materials consisted of γ-cyclodextrin derivatives dissolved in a polysiloxane matrix.[235] Polymer emulsions were used to create porous coatings on TSM resonators, and the porous polymers were subsequently coated with a variety of lipids.[236]

In 1989 Nakamoto, Moriizumi, and co-workers used an array of six TSM resonators coated with both polymeric and nonpolymeric materials to analyze 11 kinds of liquors.[237] Neural networks were 73% successful in categorizing the liquors. In another study, 8 coating materials were selected from a library of 18, in an attempt to find an optimized array. This array was used to discriminate 10 whiskys.[238,239] Flavors and fragrances were also studied.[240,241]

One group has used polymer and nonpolymer films that were applied via radio frequency sputtering of the materials.[242,243] Plasma-deposited organic films have properties significantly different from the original polymers because of the loss of atoms and fragments and the presence of dangling bonds in the deposited film. Conducting polymers have also been used as TSM resonator coating materials.[244−246]

There has been a second study on the discrimination of enantiomers.[247] Another compared the responses of a TSM resonator-based nose to those of human subjects.[248] Other examples of TSM resonator-based noses have also been studied.[249−252]

C. SAW Arrays

The first application of pattern recognition methods to data from an array of SAW devices was by Grate and co-workers in 1986.[253] A total of 12 different sensor coatings were exposed to 11 vapors. Principal components analysis was used to display in two dimensions the separation of various analytes. Hierarchical clustering categorized both the vapors and the sensor coatings. Clusterings were rationalized through their solubility parameters, including hydrogen bonding donor and acceptor ability and dipolarity/polarizability. On the basis of the classification methods used, four coatings were selected that could completely separate two classes of vapors. Mixtures of analytes were also studied.[254] An array

of four temperature-controlled SAW devices successfully detected and classified organophosphorus and organosulfur vapors.[255]

A total of 20 polymers on SAW devices were exposed to 5 organic vapors.[256] Three of the sensors were exposed to ternary mixtures of toluene, acetone, and dichloromethane. Partial least squares regression predicted the vapor concentrations, with errors of a few percent. In another study, four sensors were used to analyze ternary mixtures of water, methanol, and automotive fuel.[257] The experimental and known methanol concentrations agreed quite well. A simple two-sensor array was able to monitor H_2O and CO_2 levels in air.[258] An array of four polymer-coated SAW devices was employed to measure small amounts of tetrachloroethylene, trichloroethylene, and methoxyfurane in humid air.[259] The samples were meant to imitate exhaled breath containing trace amounts of organic contaminants; actual breath samples spiked with one of the analytes were also examined. Limits of detection were estimated to be 0.7, 0.6, and 4 ppm for tetrachloroethylene, trichloroethylene, and methoxyflurane, respectively. In a follow-up to this work, several adsorbents were tested as desorbable preconcentrators to increase the response to organic vapors in simulated exhaled breath.[260]

A combination of plasma-polymerized films, plasma-grafted films, and self-assembled monolayers was applied to SAW devices, and they were exposed to a variety of organic vapors.[261] The newly developed visually empirical region-of-influence (VERI) pattern recognition algorithm was used to analyze and categorize the data. The authors found that the best three-film array comprised one coating from each category, while the optimal arrays consisted of five to seven sensors. The same group has investigated the use of dendrimers as sensor coatings.[262]

The effects of temperature and humidity on arrays of polymer-coated SAW sensors have been studied.[263,264] Ultraviolet light-cross-linked polysiloxanes were found to have better long-term stability than noncross-linked polysiloxanes.[265]

Arrays of SAW devices coated with nonpolymeric materials have also been investigated, including liquid crystals,[266] Langmuir−Blodgett-deposited phospholipids and fatty acids,[267] self-assembled monolayers,[268] covalently bound organic molecules,[269] crown ethers,[270] and other nonvolatile organic molecules.[271]

D. Response Prediction

The frequency change of a TSM or SAW device depends on how much vapor is absorbed by the polymer film, which in turn is proportional to K, the polymer−vapor partition coefficient of the analyte. The frequency response of polymer-coated SAW resonators was predicted on the basis of the analyte's boiling point, solubility parameter, and linear solvation energy relationships.[272] The expected linear correlation was observed between log K and the vapor's boiling point, although the correlation was not as good for polar coatings. A modification of the predictions on the basis of the solvation parameters in linear solvation energy relationships (LSERs) gave the best results. Grate, Abraham, and co-workers have also extensively utilized LSERs in the prediction of sensor responses.[273−275] Hydrogen bond acidic polymers have been used specifically to improve detection and discrimination of basic vapors.[276] Other molecular orbital and molecular mechanics parameters have been used to predict SAW sensor responses.[277]

It has been found that, under certain conditions, SAW devices do not act solely as gravimetric sensors but also respond to the modulus change in polymers when a vapor is sorbed.[278] For thin films with low modulus, both SAW and TSM devices act only as gravimetric sensors, while, for polymers with initially high modulus, the SAW devices are also sensitive to the modulus change, but TSM resonators still act primarily as gravimetric sensors.[279,280] Under certain conditions, TSM resonators are also sensitive to modulus changes.[280]

Once a method for estimating responses is established, it is possible to choose the best array of sensors for detecting specific analytes or mixtures of analytes. Monte Carlo simulations of sensor responses allowed such a selection.[281]

Only one paper has been published that compares the actual analytical performance of polymer-coated TSM and SAW resonators.[282] TSM devices with frequencies of 10 and 30 MHz and SAW resonators with frequencies of 80 and 433 MHz were investigated. The influences of temperature and film thickness were studied. For each device, the thickest coating that could be applied without quenching the oscillation was applied, since thicker coatings will provide larger responses. The higher the frequency of the resonator, the less polymer could be applied. The 30 MHz TSM device had the best signal-to-noise ratio (S/N) and limits of detection (LOD) for the two polymers and two analytes that were tested.

The LOD (where $S/N = 3$) for n-octane for the 30 MHz TSM device and the 80 MHz SAW device coated with poly(dimethylsiloxane) was determined to be 2 ppm.[282] The other coating, poly(ether urethane), had LODs of 3−15 ppm. A comparable LOD of 0.6 ppm was found for n-octane on the carbon black−polymer composite nose (for the best detector in the array).[137]

IX. Conclusions and Future Prospects

Cross-reactive chemical sensor arrays are a promising alternative to conventional chemical sensors. By relying on patterns of response over a multisensor array, such systems have reduced the need to obtain the exquisite specificity of conventional sensors. The "electronic nose" or "artificial nose" moniker that has been given to such systems stems from the use of pattern recognition applied to the complex signals derived from the arrays. While not entirely misnomers, these terms do not do justice to the remarkable process of biological olfaction. Mammalian olfactory systems are continuously replacing dead cells while maintaining fidelity of the intricate neural wiring necessary to conserve responses. Signal amplification is a signature of such systems with multiples at each stage in the signal transduction process. The geometric complexity of turbinates in the nasal epithelium, the complex sniffing patterns when

animals are exposed to odors, and the convergence of similar receptor cell axons onto the olfactory bulb as well as the complex "wiring" patterns of the processing anatomy all contribute to the high sensitivity and discriminating power of the mammalian olfactory system. The systems described in this review are only rudimentary mimics of the biological system. By continuing to incorporate the operating principles of biological systems into the artificial ones, chemists may eventually be able to approach some of the capabilities of the olfactory system with these cross-reactive arrays.

As discussed in the review, there are many important and potentially exciting areas where existing arrays are beginning to have an impact. In particular, the food processing industry is relying increasingly on electronic nose systems to make determinations about quality and freshness. In addition, these industries are evaluating packaging material before adding products to make sure that such materials do not impart an off taste or odor to the food. One can imagine that as such systems get smaller, they will begin to show up as consumer items for evaluating meat, fish and dairy freshness in the kitchen as well as for monitoring potential home and workplace hazards. Such systems, by nature of their broad-bandedness, could be used for chemical and/or biological weapons detection; they could be anticipatory in the sense that they would not necessarily be keyed to particular agents but could look for responses likely to be correlated with toxicity or virulence. One day, such systems may be used to perform medical diagnostics using a simple breath test. More far-fetched, but within the realm of possibility, perhaps they may be used to recognize individuals by their signature odors. After all, dogs are able to recognize their owners by odor cues.

For purposes of discussion, this review deliberately separated the different sensor transduction mechanisms. Each of these different mechanisms offers potentially unique information about the samples being tested. The basis for the discriminating power of these arrays is the information content contained in the responses. In the ultimate manifestation of the technology, it is likely that hybrid systems will be of value because they offer the most information-rich signals.

Finally, before such systems can have a major impact, they must be manufacturable in large quantities. Because such systems rely on training computational networks on sensor response patterns, there is a need to maintain robust responses over extended time periods, otherwise retraining will be required as sensors change. Similarly, sensors must be able to be manufactured reproducibly and in large quantities so that training is transferable from one array to the next. The oldest of all chemical sensors is the pH electrode, yet today's pH electrodes are a long way from meeting such a requirement-they must be calibrated regularly (ideally before each use). Thus, there are practical impediments that must be overcome before these devices are used as routine analytical systems.

X. Acknowledgments

We acknowledge the Army Research Office, NASA, and DARPA for support of sensor array work at Caltech and acknowledge DARPA, the Office of Naval Research, the National Institutes of Health, and the Department of Energy for support at Tufts that made preparation of this review, along with some of the examples discussed herein, possible.

XI. References

(1) Elghanian, R.; Storhoff, J. J.; Mucic, R. C.; Letsinger, R. L.; Mirkin, C. A. *Science* **1997**, *277*, 1078.
(2) Göpel, W. *Mikrochim. Acta* **1997**, *125*, 179.
(3) Göpel, W. *Microelectron. Eng.* **1996**, *32*, 75.
(4) Zhu, S. S.; Carroll, P. J.; Swager, T. M. *J. Am. Chem. Soc.* **1996**, *118*, 8713.
(5) Rickert, J.; Weiss, T.; Göpel, W. *Sens. Actuators B* **1996**, *31*, 45.
(6) Schierbaum, K. D. *Sens. Actuators B* **1994**, *18*, 71.
(7) Buck, L. B.; Axel, R. *Cell* **1991**, *65*, 175.
(8) Malnic, B.; Hirono, J.; Sato, T.; Buck, L. B. *Cell* **1999**, *96*, 713.
(9) Axel, R. *Sci. Am.* **1995**, *273*, 154.
(10) Breer, H.; Wanner, I.; Strotmann, J. *Behav. Genet.* **1996**, *26*, 209.
(11) Lancet, D.; Ben-Arie, N. *Curr. Biol.* **1993**, *3*, 668.
(12) Ostrowski, J. C.; Kjelsberg, M. A.; Caron, M. G.; Lefkowitz, R. J. *Annu. Rev. Pharmacol. Toxicol.* **1992**, *32*, 167.
(13) Bartlett, P. N.; Gardner, J. W. *NATO Advanced Research Workshop on Sensors and Sensory Systems for an Electronic Nose*, Reykjavik, Iceland, 1991; Plenum Press: New York, 1991; p 31.
(14) Shimizu, Y.; Egashira, M. *MRS Bull.* **1999**, *24*(*6*), 18.
(15) Hartman, J. *Proc. Am. Soc. Hortic. Sci.* **1954**, *64*, 335.
(16) Persaud, K. C.; Dodd, G. H. *Nature* **1982**, *299*, 352.
(17) Gardner, J. W.; Bartlett, P. N. *Electronic Noses Principles and Applications*; Oxford University Press: Oxford, U.K., 1999.
(18) Gutierrez, J.; Getino, J.; Horrillo, M. C.; Ares, L.; Robla, J. I.; Garcia, C.; Sayago, I. *Thin Solid Films* **1998**, *317*, 429.
(19) Mishra, V. N.; Agarwal, R. P. *Microelectron. J.* **1998**, *29*, 861.
(20) Di Natale, C.; Davide, F. A. M.; Faglia, G.; Nelli, P. *Sens. Actuators B* **1995**, *B23*, 187.
(21) Heilig, A.; Barsan, N.; Weimar, U.; Schweizer-Berberich, M.; Gardner, J. W.; Göpel, W. *Sens. Actuators B* **1997**, *43*, 45.
(22) Corcoran, P.; Lowery, P.; Anglesea, J. *Sens. Actuators B* **1998**, *48*, 448.
(23) Doleman, B. J.; Lonergan, M. C.; Severin, E. J.; Vaid, T. P.; Lewis, N. S. *Anal. Chem.* **1998**, *70*, 4177.
(24) Gardner, J. W.; Pike, A.; Rooij, N. F.; Koudelka-Hep, M.; Clerc, P. A.; Hierlemann, A.; Göpel, W. *Sens. Actuators B* **1995**, *26*−*27*, 135.
(25) Gotz, A.; Gracia, I.; Cane, C.; Lora-Tamayo, E.; Horillo, M. C.; Getino, J.; Garcia, C.; Gutierrez, J. *Sens. Actuators B* **1997**, *44*, 483.
(26) Gardner, J. W.; Shurmer, H. V.; Corcoran, P. *Sens. Actuators B* **1991**, *B4*, 117.
(27) Hong, H.-K.; Shin, H. W.; Park, H. S.; Yun, D. H.; Kwon, C. H.; Lee, K.; Kim, S.-T.; Moriizumi, T. *Sens. Actuators B* **1996**, *33*, 68.
(28) Wang, X. D.; Yee, S.; Carey, P. *Sens. Actuators B* **1993**, *13*, 458.
(29) Bednarczyk, D.; DeWeerth, S. P. *Sens. Actuators B* **1995**, *27*, 271.
(30) Wilson, D. M.; DeWeerth, S. P. *Sens. Actuators B* **1995**, *28*, 123.
(31) Wilson, D. M.; Deweerth, S. P. *Sens. Mater.* **1998**, *10*, 169.
(32) Chaturvedi, A.; Mishra, V. N.; Dwivedi, R.; Srivastava, S. K. *Microelectron. J.* **1999**, *30*, 259.
(33) Srivastava, R.; Dwivedi, R.; Srivastava, S. K. *Sens. Actuators B* **1998**, *50*, 175.
(34) Di Natale, C.; D'Amico, A.; Davide, F. A. M.; Faglia, G.; Nelli, P.; Sberveglieri, G. *Sens. Actuators B* **1994**, *20*, 217.
(35) Getino, J.; Gutierrez, J.; Ares, L.; Robla, J. I.; Horrillo, M. C.; Sayago, I.; Agapito, J. A. *Sens. Actuators B* **1996**, *33*, 128.
(36) Abe, H.; Yoshimura, T.; Kanaya, S.; Takahashi, Y.; Miyashita, Y.; Sasaki, S. *Anal. Chim. Acta* **1987**, *194*, 1.
(37) Getino, J.; Horrillo, M. C.; Gutierrez, J.; Ares, L.; Robla, J. I.; Garcia, C.; Sayago, I. *Sens. Actuators B* **1997**, *43*, 200.
(38) Haswell, S. J.; Walmsley, A. D. *Anal. Proc.* **1991**, *28*, 115.
(39) Llobet, E.; Brezmes, J.; Vilanova, X.; Sueiras, J. E.; Correig, X. *Sens. Actuators B* **1997**, *41*, 13.
(40) Shurmer, H. V.; Gardner, J. W.; Corcoran, P. *Sens. Actuators B* **1990**, *1*, 256.
(41) Walmsley, A. D.; Haswell, S. J.; Metcalfe, E. *Anal. Chim. Acta* **1991**, *250*, 257.
(42) Walmsley, A. D.; Haswell, S. J.; Metcalfe, E. *Anal. Chim. Acta* **1991**, *242*, 31.

(43) Alexander, P. W.; Di Benedetto, L. T.; Hibbert, D. B. *Field Anal. Chem. Technol.* **1998**, *2*, 145.
(44) Di Natale, C.; Davide, F. A. M.; D′Amico, A.; Sberveglieri, G.; Nelli, P.; Faglia, G.; Perego, C. *Sens. Actuators B* **1995**, *25*, 801.
(45) Di Natale, C.; Davide, F. A. M.; D′Amico, A.; Nelli, P.; Groppelli, S.; Sberveglieri, G. *Sens. Actuators B* **1996**, *33*, 83.
(46) Gardner, J. W. *Sens. Actuators B* **1991**, *4*, 109.
(47) Gardner, J. W.; Shurmer, H. V.; Tan, T. T. *Sens. Actuators B* **1992**, *6*, 71.
(48) Llobet, E.; Hines, E. L.; Gardner, J. W.; Franco, S. *Meas. Sci. Technol.* **1999**, *10*, 538.
(49) Olafsson, R.; Martinsdottir, E.; Olafsdottir, G.; Sigfusson, P. I.; Gardner, J. W. *NATO Advanced Research Workshop on Sensors and Sensory Systems for an Electronic Nose*, Reykjavik, Iceland, 1991; Plenum Press: New York, 1991; p 257.
(50) Winquist, F.; Hornsten, E.; Sundgren, H.; Lundström, I. *Meas. Sci. Technol.* **1993**, *4*, 1493.
(51) Ulmer, H.; Mitrovics, J.; Noetzel, G.; Weimar, U.; Göpel, W. *Sens. Actuators B* **1997**, *43*, 24.
(52) Winquist, F.; Sundgren, H.; Lundström, I. *Spec. Publ.—R. Soc. Chem.* **1998**, *167*, 170.
(53) Borjesson, T.; Eklov, T.; Jonsson, A.; Sundgren, H.; Schurer, J. *Cereal Chem.* **1996**, *73*, 457.
(54) Faglia, G.; Bicelli, F.; Sberveglieri, G.; Maffezzoni, P.; Gubian, P. *Sens. Actuators B* **1997**, *44*, 517.
(55) Gardner, J. W.; Hines, E. L.; Tang, H. C. *Sens. Actuators B* **1992**, *9*, 9.
(56) Nayak, M. S.; Dwivedi, R.; Srivastava, S. K. *Sens. Actuators B* **1993**, *12*, 103.
(57) Moore, S. W.; Gardner, J. W.; Hines, E. L.; Göpel, W.; Weimar, U. *Sens. Actuators B* **1993**, *16*, 344.
(58) Marco, S.; Ortega, A.; Pardo, A.; Samitier, J. *IEEE Trans. Instrum. Meas.* **1998**, *47*, 316.
(59) Davide, F. A. M.; Di Natale, C.; D'Amico, A. *Sens. Actuators B* **1994**, *18—19*, 244.
(60) Vlachos, D. S.; Avaritsiotis, J. N. *Sens. Actuators B* **1996**, *33*, 77.
(61) Lundström, I.; Shivaraman, M. S.; Svenson, C. S.; Lundkvist, L. *Appl. Phys. Lett.* **1975**, *26*, 55.
(62) Bergveld, P. *Sens. Actuators* **1985**, *8*, 109.
(63) Vlasov, Y. G. *Mikrochim. Acta* **1991**, *2*, 363.
(64) Lundström, I.; Hedborg, E.; Spetz, A.; Sundren, H.; Winquist, F. NATO *Advanced Research Workshop on Sensors and Sensory Systems for an Electronic Nose*, Reykjavik, Iceland, 1991; Plenum Press: New York, 1991; p 303.
(65) Winquist, F.; Sundgren, H.; Hedborg, E.; Spetz, A.; Lundström, I. *Sens. Actuators B* **1992**, *B6*, 157.
(66) Muller, R.; Lange, E. *Sens. Actuators* **1986**, *9*, 39.
(67) Sundgren, H.; Lundström, I.; Winquist, F.; Lukkari, I.; Carlsson, R.; Wold, S. *Sens. Actuators B* **1990**, *2*, 115.
(68) Gall, M.; Muller, R. *Sens. Actuators* **1989**, *17*, 583.
(69) Sundgren, H.; Winquist, F.; Lukkari, I.; Lundström, I. *Meas. Sci. Technol.* **1991**, *2*, 464.
(70) Sundgren, H.; Lundström, I.; Vollmer, H. *Sens. Actuators B* **1992**, *9*, 127.
(71) Sommer, V.; Tobias, P.; Kohl, D.; Sundgren, H.; Lundström, I. *Sens. Actuators B* **1995**, *28*, 217.
(72) Lundström, I.; Erlandsson, R.; Frykman, U.; Hedborg, E.; Spetz, A.; Sundgren, H.; Welin, S.; Winquist, F. *Nature* **1991**, *352*, 47.
(73) Lundström, I.; Sundgren, H.; Winquist, F. *J. Appl. Phys.* **1993**, *74*, 6953.
(74) Eklov, T.; Sundgren, H.; Lundström, I. *Sens. Actuators B* **1997**, *45*, 71.
(75) Eklov, T.; Lundström, I. *Anal. Chem.* **1999**, *71*, 3544.
(76) www.alpha-mos.com.
(77) www.eev.com.
(78) Holmberg, M.; Winquist, F.; Lundström, I.; Gardner, J. W.; Hines, E. L. *Sens. Actuators B* **1995**, *27*, 246.
(79) Mandenius, C.-F.; Hagman, A.; Dunas, F.; Sundgren, H.; Lundström, I. *Biosens. Bioelectron.* **1998**, *13*, 193.
(80) Mandenius, C.-F.; Liden, H.; Ekloev, T.; Taherzadeh, M. J.; Liden, G. *Biotechnol. Prog.* **1999**, *15*, 617.
(81) Reddinger, J. L.; Reynolds, J. R. *Adv. Polym. Sci.* **1999**, *145*, 57.
(82) *Handbook of Conducting Polymers*; 2nd ed.; Skotheim, T. A., Elsenbaumer, R. L., Reynolds, J. R., Eds.; Marcel Dekker: New York, 1998; Vol. 1.
(83) Roncali, J. *Chem. Rev.* **1992**, *92*, 711.
(84) Epstein, A. J.; Macdiarmid, A. G. *Makromol. Chem. Macromol. Symp.* **1991**, *51*, 217.
(85) Jahnke, S. A.; Niemann, J.; Kautek, W.; Bischoff, R.; Pfeiffer, C.; Kossmehl, G. *Int. J. Environ. Anal. Chem.* **1997**, *67*, 223.
(86) Svetlicic, V.; Schmidt, A. J.; Miller, L. L. *Chem. Mater.* **1998**, *10*, 3305.
(87) www.aromascan.com.
(88) www.bloodhound.co.uk.
(89) www.zelana.com.
(90) Swann, M. J.; Glidle, A.; Cui, L.; Barker, J. R.; Cooper, J. M. *J. Chem. Soc., Chem. Commun.* **1998**, 2753.
(91) Partridge, A. C.; Harris, P. D.; Andrews, M. K. *Analyst* **1996**, *121*, 1349.
(92) Gardner, J. W.; Bartlett, P. N. *Sens. Actuators A* **1995**, *51*, 57.
(93) Gardner, J. W.; Pike, A.; de Rooij, N. F.; Koudelka-Hep, M.; Clerc, P. A.; Hierlemann, A.; Göpel, W. *Sens. Actuators B* **1995**, *26*, 135.
(94) Hodgins, D. M. *Sens. Actuators B* **1995**, *27*, 255.
(95) Slater, J. M.; Paynter, J.; Watt, E. J. *Analyst* **1993**, *118*, 379.
(96) Slater, J. M.; Watt, E. J.; Freeman, N. J.; May, I. P.; Weir, D. J. *Analyst* **1992**, *117*, 1265.
(97) Bartlett, P. N.; Gardner, J. W.; Whitaker, R. G. *Sens. Actuators A* **1990**, *23*, 911.
(98) De Wit, M.; Vanneste, E.; Geise, H. J.; Nagels, L. J. *Sens. Actuators B* **1998**, *50*, 164.
(99) Baldacci, S.; Matsuno, T.; Toko, K.; Stella, R.; De Rossi, D. *Sens. Mater.* **1998**, *10*, 185.
(100) Kawai, T.; Kojima, S.; Tanaka, F.; Yoshino, K. *Jpn. J. Appl. Phys., Part 1* **1998**, *37*, 6237.
(101) Pearce, T. C.; Gardner, J. W.; Friel, S.; Bartlett, P. N.; Blair, N. *Analyst* **1993**, *118*, 371.
(102) Hatfield, J. V.; Neaves, P.; Hicks, P. J.; Persaud, K. C.; Travers, P. J. *Sens. Actuators B* **1994**, *18*, 221.
(103) Serra, G.; Stella, R.; De Rossi, D. *Mater. Sci. Eng., C* **1998**, *5*, 259.
(104) Hodgins, D. M.; Simmonds, D. J. *J. Autom. Chem.* **1995**, *17*, 179.
(105) Bailey, T. P.; Hammond, R. V.; Persaud, K. C. *J. Am. Soc. Brew. Chem.* **1995**, *53*, 39.
(106) Gardner, J. W.; Pearce, T. C.; Friel, S.; Bartlett, P. N.; Blair, N. *Sens. Actuators B* **1994**, *18*, 240.
(107) Pearce, T. C.; Gardner, J. W. *Analyst* **1998**, *123*, 2047.
(108) Cantalejo, M. J. *Z. Lebensmittel Untersuchung Forschung A* **1999**, *208*, 373.
(109) Schaller, E.; Bosset, J. O.; Escher, F. *Chimia* **1999**, *53*, 98.
(110) Annor-Frempong, I. E.; Nute, G. R.; Wood, J. D.; Whittington, F. W.; West, A. *Meat Sci.* **1998**, *50*, 139.
(111) Gibson, T. D.; Prosser, O. C.; Hulbert, J. N.; Marshall, R. W.; Corcoran, P.; Lowery, P.; Ruck-Keene, E. A.; Heron, S. *Sens. Actuators B* **1997**, *44*, 413.
(112) Arnold, J. W.; Senter, S. D. *J. Sci. Food Agric.* **1998**, *78*, 343—348.
(113) Stuetz, R. M.; Fenner, R. A.; Engin, G. *Water Res.* **1999**, *33*, 453.
(114) Stuetz, R. M.; Fenner, R. A.; Engin, G. *Water Res.* **1999**, *33*, 442.
(115) Stuetz, R. M.; White, M.; Fenner, R. A. *J. Water Serv. Res. Technol.-Aqua* **1998**, *47*, 223.
(116) Stuetz, R. M.; Engin, G.; Fenner, R. A. *Water Sci. Technol.* **1998**, *38*, 331.
(117) Persaud, K. C.; Khaffaf, S. M.; Hobbs, P. J.; Sneath, R. W. *Chem. Senses* **1996**, *21*, 495.
(118) Byun, H. G.; Persaud, K. C.; Khaffaf, S. M.; Hobbs, P. J.; Misselbrook, T. H. *Comput. Electron. Agric.* **1997**, *17*, 233.
(119) Misselbrook, T. H.; Hobbs, P. J.; Persaud, K. C. *J. Agr. Eng. Res.* **1997**, *66*, 213.
(120) Masila, M.; Sargent, A.; Sadik, O. A. *Electroanalysis* **1998**, *10*, 312.
(121) Lane, A. J. P.; Wathes, D. C. *J. Dairy Sci.* **1998**, *81*, 2145.
(122) Schiffman, S. S.; Kermani, B. G.; Nagle, H. T. *Chem. Senses* **1997**, *22*, 119.
(123) Chandiok, S.; Crawley, B. A.; Oppenheim, B. A.; Chadwick, P. R.; Higgins, S.; Persaud, K. C. *J. Clin. Path.* **1997**, *50*, 790.
(124) Persaud, K. C.; Pisanelli, A. M.; Szyszko, S.; Reichl, M.; Horner, G.; Rakow, W.; Keding, H. J.; Wessels, H. *Sens. Actuators B* **1999**, *55*, 118.
(125) Amrani, M. E. H.; Ibrahim, M. S.; Persaud, K. C. *Mater. Sci. Eng.* **1993**, *C1*, 17.
(126) Amrani, M. E. H.; Persaud, K. C.; Payne, P. A. *Meas. Sci. Technol.* **1995**, *6*, 1500.
(127) Amrani, M. E. H.; Payne, P. A.; Persaud, K. C. *Sens. Actuators B* **1996**, *33*, 137.
(128) Amrani, M. E. H.; Dowdeswell, R. M.; Payne, P. A.; Persaud, K. C. *Sens. Actuators B* **1997**, *44*, 512.
(129) Amrani, M. E. H.; Payne, P. A. *IEE Proc. Sci. Meas. Technol.* **1999**, *146*, 95.
(130) Lonergan, M. C.; Severin, E. J.; Doleman, B. J.; Beaber, S. A.; Grubb, R. H.; Lewis, N. S. *Chem. Mater.* **1996**, *8*, 2298.
(131) Freund, M. S.; Lewis, N. S. *Proc. Natl. Acad. Sci. U.S.A.* **1995**, *92*, 2652.
(132) Brosseau, C.; Boulic, F.; Queffelec, P.; Bourbigot, C.; LeMest, Y.; Loaec, J.; Beroual, A. *J. Appl. Phys.* **1997**, *81*, 882.
(133) Kirkpatrick, S. R. *Rev. Mod. Phys.* **1973**, *45*, 574.
(134) Doleman, B. J.; Sanner, R. D.; Severin, E. J.; Grubbs, R. H.; Lewis, N. S. *Anal. Chem.* **1998**, *70*, 2560.
(135) Severin, E. J.; Sanner, R. D.; Doleman, B. J.; Lewis, N. S. *Anal. Chem.* **1998**, *70*, 1440.
(136) Doleman, B. J.; Severin, E. J.; Lewis, N. S. *Proc. Natl. Acad. Sci. U.S.A.* **1998**, *95*, 5442.
(137) Doleman, B. J. Ph.D., California Institute of Technology, 1999.
(138) Seitz, W. R. *Crit. Rev. Anal. Chem.* **1988**, *19*, 135.
(139) Dickinson, T. A.; White, J.; Kauer, J. S.; Walt, D. R. *Trends Biotechnol.* **1998**, *16*, 250.

(140) Steemers, F. J.; Walt, D. R. *Mikrochim. Acta* **1999**, *131*, 99.
(141) Barnard, S. M.; Walt, D. R. *Nature* **1991**, *353*, 338.
(142) Orellana, G.; Gomez-Carneros, A.; de Dios, C.; Garcia-Martinez, A.; Moreno-Bondi, M. *Anal. Chem.* **1995**, *67*, 2231.
(143) Posch, H. E.; Wolfbeis, O. S.; Pusterhoffer, J. *Talanta* **1988**, *35*, 89.
(144) Ronot, C.; Archenault, M.; Gagnaire, H.; Goure, J. P.; Jaffrezic-Renault, N.; Pichery, T. *Sens. Actuators B* **1993**, *11*, 375.
(145) Ronot, C.; Gagnaire, H.; Goure, J. P.; Jaffrezic-Renault, N.; Pichery, T. *Sens. Actuators A* **1994**, *42*, 529.
(146) Gauglitz, G.; Kraus, G. *Fresenius' J. Anal. Chem.* **1993**, *346*, 572.
(147) Dickert, F. L.; Keppler, M. *Adv. Mater.* **1995**, *7*, 1020.
(148) Walt, D. R.; Dickinson, T.; White, J.; Kauer, J.; Johnson, S.; Engelhardt, H.; Sutter, J. M.; Jurs, P. C. *Biosens. Bioelectron.* **1998**, *13*, 695.
(149) Pantano, P.; Walt, D. R. *Anal. Chem.* **1995**, *67*, 481A.
(150) Dickinson, T. A.; White, J.; Kauer, J. S.; Walt, D. R. *Nature* **1996**, *382*, 697.
(151) White, J.; Kauer, J. S.; Dickinson, T. A.; Walt, D. R. *Anal. Chem.* **1996**, *68*, 2191.
(152) Albert, K. J.; Walt, D. R. *Anal. Chem.* **2000**, *72*, 1947.
(153) Micheal, K. L.; Taylor, L. C.; Schultz, S. L.; Walt, D. R. *Anal. Chem.* **1998**, *70*, 1242.
(154) Dickinson, T. A.; Michael, K. L.; Kauer, J. S.; Walt, D. R. *Anal. Chem.* **1999**, *71*, 2192.
(155) Lavigne, J. J.; Savoy, S.; Clevenger, M. B.; Ritchie, J. E.; McDoniel, B.; Yoo, S.-J.; Anslyn, E. V.; McDevitt, J. T.; Shear, J. B.; Neikirk, D. *J. Am. Chem. Soc.* **1998**, *120*, 6429.
(156) Healey, B. G.; Walt, D. R. *Anal. Chem.* **1997**, *69*, 2213.
(157) Sutter, J. M.; Jurs, P. C. *Anal. Chem.* **1997**, *69*, 856.
(158) Otto, M.; Thomas, J. D. R. *Anal. Chem.* **1985**, *57*, 2647.
(159) Beebe, K. R.; Uerz, D.; Sandifer, J.; Kowalski, B. R. *Anal. Chem.* **1988**, *60*, 66.
(160) Beebe, K. R.; Kowalski, B. R. *Anal. Chem.* **1988**, *60*, 2272.
(161) Bos, M.; Bos, A.; van der Linden, W. E. *Anal. Chim. Acta* **1990**, *233*, 31.
(162) Forster, R. J.; Regan, F.; Diamond, D. *Anal. Chem.* **1991**, *63*, 876.
(163) Forster, R. J.; Diamond, D. *Anal. Chem.* **1992**, *64*, 1721.
(164) Diamond, D.; Forster, R. J. *Anal. Chim. Acta* **1993**, *276*, 75.
(165) Legin, A. V.; Vlasov, Y. G.; Rudnitskaya, A. M.; Bychkov, E. A. *Sens. Actuators B* **1996**, *34*, 456.
(166) Stetter, J. R.; Jurs, P. C.; Rose, S. L. *Anal. Chem.* **1986**, *58*, 860.
(167) Stetter, J. R.; Findlay, M. W.; Maclay, G. J.; Zhang, J.; Vaihinger, S.; Göpel, W. *Sens. Actuators B* **1990**, *1*, 43.
(168) Vaihinger, S.; Göpel, W.; Stetter, J. R. *Sens. Actuators B* **1991**, *4*, 337.
(169) Stetter, J. R.; Findlay, M. W. J.; Schroeder, K. M.; Yue, C.; Penrose, W. R. *Anal. Chim. Acta* **1993**, *284*, 1.
(170) Schweizer-Berberich, P.-M.; Vaihinger, S.; Göpel, W. *Sens. Actuators B* **1994**, *18*, 282−290.
(171) Wang, J.; Rayson, G. D.; Lu, Z.; Wu, H. *Anal. Chem.* **1990**, *62*, 1924.
(172) Glass, R. S.; Perone, S. P.; Ciarlo, D. R. *Anal. Chem.* **1990**, *62*, 1914.
(173) Chen, Q.; Wang, J.; Rayson, G.; Tian, B.; Lin, Y. *Anal. Chem.* **1993**, *65*, 251.
(174) Wehrens, R.; van der Linden, W. E. *Anal. Chim. Acta* **1996**, *334*, 93.
(175) Yang, Z.; Sasaki, S.; Karube, I.; Suzuki, H. *Anal. Chim. Acta* **1997**, *357*, 41.
(176) Ross, B.; Cammann, K.; Mokwa, W.; Rospert, M. *Sens. Actuators B* **1992**, *7*, 758.
(177) Atkinson, J. K.; Shahi, S. S.; Varney, M.; Hill, N. *Sens. Actuators B* **1991**, *4*, 175.
(178) Augelli, M.; Nascimento, V. B.; Pedrotti, J. J.; Gutz, I. G. R.; Angnes, L. *Analyst* **1997**, *122*, 843.
(179) Kounaves, S. P.; Deng, W.; Hallock, P. R.; Kovacs, G. T. A.; Storment, C. W. *Anal. Chem.* **1994**, *66*, 418.
(180) Kovacs, G. T. A.; Storment, C. W.; Kounaves, S. P. *Sens. Actuators B* **1995**, *23*, 41.
(181) Reay, R.; Flannery, A. F.; Storment, C. W.; Kounaves, S. P.; Kovacs, G. T. A. *Sens. Actuators B* **1996**, *34*, 450.
(182) Uhlig, A.; Schnakenberg, U.; Hintsche, R. *Electroanalysis* **1997**, *9*, 125.
(183) Paeschke, M.; Dietrich, F.; Uhlig, A.; Hintsche, R. *Electroanalysis* **1996**, *8*, 891.
(184) Silva, P. R. M.; El Khakani, M. A.; Chaker, M.; Champagne, G. Y.; Chevalet, J.; Gastonguay, L.; Lacasse, R.; Ladouceur, M. *Anal. Chim. Acta* **1999**, *385*, 249.
(185) Feeney, R.; Herdan, J.; Nolan, M. A.; Tan, S. H.; Tarasov, V.; Kounaves, S. P. *Electroanalysis* **1998**, *10*, 1.
(186) Belmont, C.; Tercier, M.-L.; Buffle, J.; Fiaccabrino, G. C.; Koudelka-Hep, M. *Anal. Chim. Acta* **1996**, *329*, 203.
(187) Herdan, J.; Feeney, R.; Kounaves, S. P.; Flannery, A. F.; Storment, C. W.; Kovacs, G. T. A.; Darling, R. B. *Environ. Sci. Technol.* **1998**, *32*, 131.
(188) Matson, W. R.; Langlais, P.; Volicer, L.; Gamache, P. H.; Bird, E.; Mark, K. A. *Clin. Chem.* **1984**, *30*, 1477.
(189) Matson, W. R.; Gamache, P. G.; Beal, M. F.; Bird, E. D. *Life Sci.* **1987**, *41*, 905.
(190) Niwa, O.; Horiuchi, T.; Morita, M.; Huang, T.; Kissinger, P. T. *Anal. Chim. Acta* **1996**, *318*, 167.
(191) Liu, J.; Zhou, W.; You, T.; Li, F.; Wang, E.; Dong, S. *Anal. Chem.* **1996**, *68*, 3350.
(192) Niwa, O.; Morita, M. *Anal. Chem.* **1996**, *68*, 355.
(193) Jin, W. R.; Weng, Q.; Wu, J. *Anal. Chim. Acta* **1997**, *342*, 67.
(194) Iwasaki, Y.; Morita, M. *Curr. Sep.* **1995**, *14*, 2.
(195) Gavin, P. F.; Ewing, A. G. *J. Am. Chem. Soc.* **1996**, *118*, 8932.
(196) Gavin, P. F.; Ewing, A. G. *Anal. Chem.* **1997**, *69*, 3838.
(197) Chao, M. H.; Huang, H. J. *Anal. Chem.* **1997**, *69*, 463.
(198) Svendsen, C. N. *Analyst* **1993**, *118*, 123.
(199) You, T.; Wu, M.; Wang, E. *Anal. Lett.* **1997**, *30*, 1025.
(200) Slater, J. M.; Watt, E. J. *Analyst* **1994**, *119*, 2303.
(201) Skladal, P.; Kalab, T. *Anal. Chim. Acta* **1995**, *316*, 73.
(202) Wollenberger, U.; Paeschke, M.; Hintsche, R. *Analyst* **1994**, *119*, 1245.
(203) Wang, J.; Chen, Q. *Anal. Chem.* **1994**, *66*, 1007.
(204) Anderson, J. L.; Coury, L. A., Jr.; Leddy, J. *Anal. Chem.* **1999**, *70*, 519R.
(205) Janata, J.; Josowicz, M.; Vanysek, P.; DeVaney, D. M. *Anal. Chem.* **1998**, *70*, 179R.
(206) Strobel, H. A.; Heineman, W. R. *Chemical Instrumentation: A Systematic Approach*; John Wiley & Sons (Wiley-Interscience): New York, 1989.
(207) Bakker, E.; Buhlmann, P.; Pretsch, E. *Chem. Rev.* **1997**, *97*, 3083.
(208) Cosofret, V. V.; Erdosy, M.; Johnson, T. A.; Buck, R. P.; Ash, R. B.; Neuman, M. R. *Anal. Chem.* **1995**, *67*, 1647.
(209) Lauks, I. R. *Acc. Chem. Res.* **1998**, *31*, 317.
(210) Skoog, D. A.; Leary, J. J. *Principles of Instrumental Analysis*; 4th ed.; ed.; Saunders College Publishers: New York, 1992.
(211) Forster, R. J.; Diamond, D. *Anal. Commun.* **1996**, *33*, 1H.
(212) Amatore, C.; Thouin, L.; Warkocz, J.-S. *Chem. Eur. J.* **1999**, *5*, 456.
(213) Grate, J. W.; Martin, S. J.; White, R. M. *Anal. Chem.* **1993**, *65*, 940A.
(214) Sauerbrey, G. *Z. Physik.* **1959**, *155*, 206.
(215) King, W. H. *Anal. Chem.* **1964**, *39*, 1735.
(216) Wohltjen, H.; Dessey, R. *Anal. Chem.* **1979**, *51*, 1458.
(217) Carey, W. P.; Beebe, K. R.; Kowalski, B. R.; Illman, D. L.; Hirschfeld, T. *Anal. Chem.* **1986**, *58*, 149.
(218) Carey, W. P.; Kowalski, B. R. *Anal. Chem.* **1986**, *58*, 3077−3084.
(219) Hirschfeld, T.; Olness, D. *Sorption Detector System for Chemical Agents Detection and Recoginition*; U.S. Army Chemical Research and Development Center:, 1984.
(220) Lorber, A. *Anal. Chem.* **1986**, *58*, 1167.
(221) Carey, W. P.; Beebe, K. R.; Kowalski, B. R. *Anal. Chem.* **1987**, *59*, 1529.
(222) Draper, N. R.; Smith, H. *Applied Regression Analysis*, 3rd ed.; Wiley: New York, 1998.
(223) Geladi, P.; Kowalski, B. R. *Anal. Chim. Acta* **1986**, *185*, 1.
(224) Carey, W. P.; Kowalski, B. R. *Anal. Chem.* **1988**, *60*, 541.
(225) Lucklum, R.; Henning, B.; Hauptmann, P.; Schierbaum, K. D.; Vaihinger, S.; Göpel, W. *Sens. Actuators A* **1991**, *25−27*, 705.
(226) Schierbaum, K. D.; Hierlmann, A.; Göpel, W. *Sens. Actuators B* **1994**, *18−19*, 448.
(227) Zhou, R.; Weimar, U.; Schierbaum, K. D.; Geckeler, K. E.; Göpel, W. *Sens. Actuators B* **1995**, *26−27*, 121.
(228) Zhou, R.; Hierlemann, A.; Schierbaum, K. D.; Geckeler, K. E.; Göpel, W. *Sens. Actuators B* **1995**, *24−25*, 443.
(229) Hierlemann, A.; Weimar, U.; Kraus, G.; Gauglitz, G.; Göpel, W. *Sensors Mater.* **1995**, *7*, 179.
(230) Hierlemann, A.; Weimar, U.; Kraus, G.; Schweizer-Berberich, M.; Göpel, W. *Sens. Actuators B* **1995**, *26−27*, 126.
(231) Schweizer-Berberich, M.; Göppert, J.; Hierlemann, A.; Mitrovics, J.; Weimar, U.; Rosenstiel, W.; Göpel, W. *Sens. Actuators B* **1995**, *26−27*, 232.
(232) Hierlemann, A.; Bodenhöfer, K.; Fluck, M.; Schurig, V.; Göpel, W. *Anal. Chim. Acta* **1997**, *346*, 327.
(233) Bodenhöfer, K.; Hierlemann, A.; Seeman, J.; Gauglitz, G.; Koppenhoefer, B.; Göpel, W. *Nature* **1997**, *387*, 577.
(234) Bodenhöfer, K.; Hierlemann, A.; Seeman, J.; Gauglitz, G.; Christian, B.; Koppenhoefer, B.; Göpel, W. *Anal. Chem.* **1997**, *69*, 3058.
(235) Bodenhöfer, K.; Hierlemann, A.; Juza, M.; Schurig, V.; Göpel, W. *Anal. Chem.* **1997**, *69*, 4017.
(236) Yano, K.; Bornscheuer, U. T.; Schmid, R. D.; Yoshitake, H.; Ji, H.-S.; Ikebukuro, K.; Masuda, Y.; Karube, I. *Biosens. Bioelectron.* **1998**, *13*, 397.
(237) Ema, K.; Yokoyama, M.; Nakamoto, T.; Moriizumi, T. *Sens. Actuators* **1989**, *18*, 291.
(238) Nakamoto, T.; Fukunishi, K.; Moriizumi, T. *Sens. Actuators B* **1990**, *1*, 473.
(239) Nakamoto, T.; Fukuda, A.; Moriizumi, T. *Sens. Actuators B* **1991**, *3*, 221.
(240) Nakamoto, T.; Fukuda, A.; Moriizumi, T. *Sens. Actuators B* **1993**, *10*, 85.

(241) Ide, J.; Nakamoto, T.; Moriizumi, T. *Sens. Actuators B* **1993**, *13*−*14*, 351.
(242) Nakamura, M.; Sugimoto, I.; Kuwano, H. *J. Intell. Mater. Syst. Struct.* **1994**, *5*, 315.
(243) Sugimoto, I.; Nakamura, M.; Kuwano, H. *Sens. Actuators B* **1996**, *37*, 163.
(244) Slater, J. M.; Watt, E. J. *Analyst* **1991**, *116*, 1125.
(245) Slater, J. M.; Watt, E. J.; Freeman, N. J.; May, I. P.; Weir, D. J. *Analyst* **1992**, *117*, 1265.
(246) Deng, Z.; Stone, D. C.; Thompson, M. *Analyst* **1996**, *121*, 671.
(247) May, I. P.; Byfield, M. P.; Lindström, M.; Wünsche, L. F. *Chirality* **1997**, *9*, 225.
(248) Yokoyama, K.; Ebisawa, F. *Anal. Chem.* **1993**, *65*, 673.
(249) Cao, Z.; Xu, D.; Jiang, J.-H.; Wang, J.-H.; Lin, H.-G.; Xu, C.-J.; Xhang, X.-B.; Yu, R.-Q. *Anal. Chim. Acta* **1996**, *335*, 117.
(250) Barkó, G.; Hlavay, J. *Talanta* **1997**, *44*, 2237.
(251) Zhang, S.; Li, S. F. Y. *Analyst* **1996**, *121*, 1721.
(252) Schmautz, A. *Sens. Actuators B* **1992**, *6*, 38.
(253) Ballantine, D. S.; Rose, S. L.; Grate, J. W.; Wohltjen, H. *Anal. Chem.* **1986**, *58*, 3058.
(254) Rose-Pehrsson, S.; Grate, J.; Ballantine, D. S.; Jurs, P. C. *Anal. Chem.* **1988**, *60*, 2801.
(255) Grate, J. W.; Rose-Pehrsson, S. L.; Venezky, D. L.; Klusty, M.; Wohltjen, H. *Anal. Chem.* **1993**, *65*, 1868.
(256) Amati, D.; Arn, D.; Blom, N.; Ehrat, M.; Saunois, J.; Widmer, H. M. *Sens. Actuators B* **1992**, *7*, 587.
(257) Reichert, J.; Coerdt, W.; Ache, H. J. *Sens. Actuators B* **1993**, *13*−*14*, 293.
(258) Hoyt, A. E.; Ricco, A. J.; Bartholomew, J. W.; Osbourn, G. C. *Anal. Chem.* **1998**, *70*, 2137.
(259) Groves, W. A.; Zellers, E. T. *Am. Ind. Hyg. Assoc. J.* **1996**, *57*, 1103.
(260) Groves, W. A.; Zellers, E. T.; Frye, G. C. *Anal. Chim. Acta* **1998**, *371*, 131.
(261) Ricco, A. J.; Crooks, R. M.; Osbourn, G. C. *Acc. Chem. Res.* **1998**, *31*, 289.
(262) Crooks, R. M.; Ricco, A. J. *Acc. Chem. Res.* **1998**, *31*, 219.
(263) Liron, Z.; Greenblatt, J.; Frishman, G.; Gratziani, N.; Biran, A. *Sens. Actuators B* **1993**, *12*, 115.
(264) Zellers, E. T.; Han, M. *Anal. Chem.* **1996**, *68*, 2409.
(265) Barié, N.; Rapp, M.; Ache, H. J. *Sens. Actuators B* **1998**, *46*, 97.
(266) Patrash, S. J.; Zellers, E. T. *Anal. Chim. Acta* **1994**, *288*, 167.
(267) Chang, S.-M.; Tamiya, E.; Karube, I.; Sato, M.; Masuda, Y. *Sens. Actuators B* **1991**, *5*, 53.
(268) Thomas, R. C.; Yang, H. C.; DiRubio, C. R.; Ricco, A. J.; Crooks, R. M. *Langmuir* **1996**, *12*, 2239.
(269) Moore, L. W.; Springer, K. N.; Shi, J.-X.; Yang, X.; Swanson, B. I.; Li, D. *Adv. Mater.* **1995**, *7*, 729.
(270) Lu, C.-J.; Shih, J.-S. *Anal. Chim. Acta* **1995**, *306*, 129.
(271) Katritzky, A. R.; Savage, G. P.; Pilarska, M. *Talanta* **1991**, *38*, 201.
(272) Patrash, S. J.; Zellers, E. T. *Anal. Chem.* **1993**, *65*, 2055.
(273) Grate, J. W.; Patrash, S. J.; Abraham, M. H. *Anal. Chem.* **1995**, *67*, 2162.
(274) Grate, J. W.; Abraham, M. H.; McGill, R. A. *Handbook of Biosensors and Electronic Noses*; Kress-Rogers, E., Ed.; CRC Press: New York, 1997.
(275) McGill, R. A.; Abraham, M. H.; Grate, J. W. *Chemtech* **1994**, *24*, 27.
(276) Grate, J. W.; Patrash, S. J.; Kaganove, S. N. *Anal. Chem.* **1999**, *71*, 1033.
(277) Slater, J. M.; Paynter, J. *Analyst* **1994**, *119*, 191.
(278) Grate, J. W.; Klusty, M.; McGill, R. A.; Abraham, M. H.; Whiting, G.; Andonian-Haftvan, J. *Anal. Chem.* **1992**, *64*, 610.
(279) Grate, J. W.; Kaganove, S. N.; Bhethanabotla, V. R. *Faraday Discuss.* **1997**, *107*, 259.
(280) Grate, J. W.; Kaganove, S. N.; Bhethanabotla, V. R. *Anal. Chem.* **1998**, *70*, 199.
(281) Zellers, E. T.; Batterman, S. A.; Han, M.; Patrash, S. J. *Anal. Chem.* **1995**, *67*, 1092.
(282) Bodenhöfer, K.; Hierlemann, A.; Noetzel, G.; Weimar, U.; Göpel, W. *Anal. Chem.* **1996**, *68*, 2210.

CR980102W